

Competing orders II: the doped quantum dimer model

Leon Balents,¹ Lorenz Bartosch,^{2,3} Anton Burkov,¹ Subir Sachdev,² and Krishnendu Sengupta²

¹*Department of Physics, University of California, Santa Barbara, CA 93106-4030*

²*Department of Physics, Yale University, P.O. Box 208120, New Haven, CT 06520-8120*

³*Institut für Theoretische Physik, Universität Frankfurt, Postfach 111932, 60054 Frankfurt, Germany*

(Dated: September 19, 2004)

We study the phases of doped spin $S = 1/2$ quantum antiferromagnets on the square lattice, as they evolve from paramagnetic Mott insulators with valence bond solid (VBS) order at doping $\delta = 0$, to superconductors at moderate δ . The interplay between density wave/VBS order and superconductivity is efficiently described by the quantum dimer model, which acts as an effective theory for the total spin $S = 0$ sector. We extend the dimer model to include fermionic $S = 1/2$ excitations, and show that its mean-field, static gauge field saddle points have projective symmetries (PSGs) similar to those of ‘slave’ particle U(1) and SU(2) gauge theories. We account for the non-perturbative effects of gauge fluctuations by a duality mapping of the $S = 0$ dimer model. The dual theory of vortices has a PSG identical to that found in a previous paper (L. Balents *et al.*, cond-mat/0408329) by a duality analysis of bosons on the square lattice. The previous theory therefore also describes fluctuations across superconducting, supersolid and Mott insulating phases of the present electronic model. Finally, with the aim of describing neutron scattering experiments, we present a phenomenological model for collective $S = 1$ excitations and their coupling to superflow and density wave fluctuations.

I. INTRODUCTION

In a previous paper¹ (hereafter referred to as I), we described the physics of two-dimensional superfluids in the vicinity of a localization transition into a commensurate Mott insulator. Our primary focus was on bosons on the square lattice, and we demonstrated the role played by the projective transformations (the PSG) of the vortices in the superfluid under operations of the square lattice space group. The present paper will extend our analysis to paired electron models on the square lattice, with the aim of justifying applicability to the cuprate superconductors. A simple physical argument based on universality was given in I clearly validating that analysis when the superconducting state neighboring the Mott insulator is an s -wave state with a large quasiparticle gap, and it was claimed that the same description also holds for a similarly gapped “strong pairing” d -wave state. In this paper, we back up this claim with detailed microscopic analysis of a set of models that incorporate local singlet formation. Specifically, we find that most of the results of I can be applied essentially unchanged, with the PSG determined by the particle density of Cooper pairs. We will also discuss the extent to which our results can be applied to “weak pairing” d -wave superconductors with gapless nodal quasiparticles.

Most of our analysis here will be carried out in the context of the quantum dimer model. This model was proposed by Rokhsar, Kivelson, and Fradkin^{2,7} as an effective theory of the $S = 0$ excitations of the insulating, paramagnetic phases of square lattice antiferromagnets. For generic parameters, the insulating dimer model has a ground state which breaks the symmetry of the square lattice space group with the development of valence bond solid (VBS) order^{3,4,5,6}. The dimer model was also extended^{2,7} to allow for $S = 0$ charged excitations:

the Hilbert space was expanded to include bosonic holes with density δ , and it was argued that the ground state is a superfluid at finite δ (the pairing symmetry of this superconducting state is somewhat unclear in these works, and will be clarified below). The doped quantum dimer model is therefore ideally suited to our primary purpose here of describing the evolution from the VBS Mott insulator to the superfluid as a function of increasing δ .

We will begin in Section II by reviewing the formulation^{7,8} of the quantum dimer model as a compact U(1) gauge theory (with gauge field \hat{A}) in the presence of a background static matter field of charges ± 1 on the two sublattices of the square lattice. Upon doping, the holes appear as two $S = 0$ dynamic bose fields $b_{i\sigma}$ (i is a square lattice site index and the index $\sigma = \pm 1$ labels the sublattice upon which the boson primarily resides). These bosons have charges σ under the compact U(1) gauge field \hat{A} .

In Section III we show how the above theory of the spin $S = 0$ sector can be extended to include $S = 1/2$ fermionic excitations f_{is} ($s = \uparrow, \downarrow$ is a spin label). These fermionic ‘spinons’ also carry unit staggered charges under the compact U(1) gauge field \hat{A} . While these fermionic excitations are gapped and confined in the undoped insulator, the structure of our theory allows these fermions to become gapless quasiparticles at nodal points in a possible d -wave superconducting ground state at finite δ : they then become the conventional $S = 1/2$ Bogoliubov quasiparticles of this superconductor. With this construction, we can directly discuss the pairing symmetry of the superfluid states of the doped dimer model. We will also consider collective $S = 1$ ‘triplon’ excitations in Section V.

So far we have mainly defined the degrees of freedom of our theory on the lattice scale, but this generally does not specify its ultimate ground state or the quantum num-

bers of its quasiparticles. In particular, we are considering a strongly interacting 2+1 dimensional compact U(1) gauge theory, and the non-perturbative fluctuations of \hat{A} must be treated with great care. Generally, for the dimer models we consider here, these fluctuations drive confinement at long scales. Nevertheless, it is useful to initially neglect gauge fluctuations and to consider mean-field saddle points with a fixed background \hat{A} . Such saddle points describe (unstable) ‘spin liquid’ states, which may be considered the progenitors of the superconducting and/or charge ordered Mott phases which appear as ground states. A subsequent treatment of gauge fluctuations describes this evolutionary descent via confinement or the Higgs mechanism. Remarkably, we will find in Section III C that, at least at the level of PSGs, the spin liquid saddle points of the dimer model are related to particular (generalized) saddle points of earlier slave-particle U(1) (Refs. 9,10) or SU(2) (Ref. 11) gauge theories. The particular saddle points appropriate to dimer models, however, are distinct from those advocated as candidate spin liquid states in the slave particle work. They have appeared – without much attention – in Wen’s PSG classification of symmetric spin liquids¹⁶ (the specific identifications of these spin liquids appear at the end of Section III C). Our work thus resolves one question posed in Ref. 16, as to how the (putative) spin liquid states of the quantum dimer model fit into this classification scheme. Beyond classification, the physical interpretation we shall give to our dimer model saddle points, and our subsequent non-perturbative treatment of gauge fluctuations, lead us eventually to conclusions on the physical properties of our theory which differ from those reached in Refs. 11,12.

There is one situation in which it is clear that the \hat{A} gauge fluctuations are relatively innocuous. This is the moderate δ state in which the $b_{i\sigma}$ are strongly condensed and the square lattice symmetry is fully preserved: the condensate acts like a Higgs field which quenches \hat{A} fluctuations. Such a state is a superconductor, and we will show in Section III D that microscopic energetic considerations and the PSG constrain the pairing symmetry of the superconductor; d - and s - wave (and other) pairings emerge under suitable conditions.

So what is the fate of this putative d -wave superconductor as δ is reduced? As noted above, we know from Refs. 3,8 that strong \hat{A} fluctuations produce a VBS insulator at $\delta = 0$, and so a careful treatment of \hat{A} fluctuations must surely become increasingly important as δ is reduced. In previous work^{10,13,14,15} on U(1) slave particle and related theories, the evolution between a finite δ d -wave superconductor and a VBS insulator at $\delta = 0$ was addressed in a mean-field theory (similar to that just discussed above) but which also allowed for breaking of the square lattice symmetry by the development of density wave/VBS order coexisting with superfluidity. This had the advantage of explicitly displaying the evolution of the gapless fermionic nodal quasiparticle excitations with decreasing δ : the nodes present at larger δ disappeared

(due to collisions in pairs at the (reduced) Brillouin zone boundaries) at a critical doping $\delta = \delta_f$, larger than the doping δ_c at which the Mott transition occurs. For small enough $\delta < \delta_c$, a fully-gapped insulating VBS state was obtained. However, this work treated gauge or VBS fluctuations in a cavalier manner, and the VBS order was static and likely overestimated in magnitude.

In the application to the cuprates, we have in mind that these insulating or supersolid states obtained in our theory at finite doping are models of the situation near doping $\delta = 1/8$. There is much experimental evidence (*e.g.* in $\text{La}_{1.6-x}\text{Nd}_{0.4}\text{Sr}_x\text{CuO}_4$ in Ref. 17) that exactly at $\delta = 1/8$ the superconductivity is strongly suppressed, and perfect long-range order with a period of 4 lattice spacings develops (as is also the case in Fig 9).

In Section IV, we will address the δ driven evolution from a VBS insulator to a superconductor in an approach which fully accounts for the non-perturbative effects of the fluctuations of \hat{A} . No previous analysis^{10,11,12,13,14,15,16} has accounted for strong gauge fluctuations in this regime. However, we will only be able to do this in the context of the $S = 0$ model of Section II: non-zero S excitations will be neglected in Section IV. While this is probably safe within the phases obtained therein, neglect of gapless nodal $S = 1/2$ fermionic excitations is likely invalid at the quantum critical points. A full treatment which synthesizes the results of Sections III and IV, and thus accounts for *both* strong \hat{A} fluctuations and gapless $S = 1/2$ fermions at quantum critical points is not available, and remains a challenging and important open problem.

The analysis of the $S = 0$ sector in Section IV is carried out by a duality mapping into a theory of vortices. The resulting effective theory for the vortices has a structure similar to the models considered in I, and can therefore be similarly classified by an analysis of the action of the PSG on the vortices. With the knowledge of the PSG, many of the results of I can be directly applied here. We will also present in Section IV B a mean-field analysis of the dual vortex theory which results in a phase diagram of the dimer model as a function of δ . It is important to note that this dual mean-field theory accounts for non-perturbative confining effects of the \hat{A} fluctuations: these are built into the duality mapping.

II. QUANTUM DIMER MODEL

This section describes the doped quantum dimer model², viewed as an effective theory of the spin $S = 0$ sector of doped quantum antiferromagnets. The resulting theory will be a compact U(1) gauge theory^{7,8} coupled to two classes of matter fields: (i) *static* charges of ± 1 on the two sublattices, and (ii) *dynamic* bosons of charges ± 1 with a total physical density δ (note: bosons of both gauge charges contribute a positive number to the physical density).

The Hamiltonian of the quantum dimer model can be

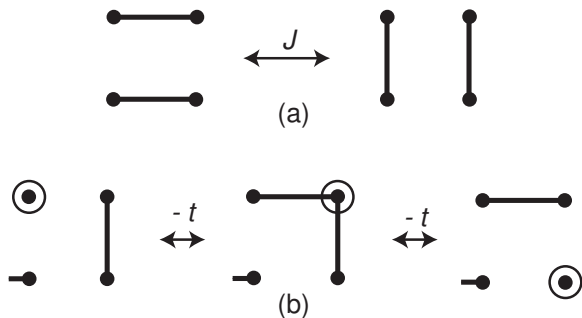


FIG. 1: Elementary moves of the quantum dimer model. (a) The resonance of two dimers around a plaquette, which occurs with amplitude J in Eq. (2.3). (b) Hopping of a hole with the amplitude t term in Eq. (2.7). The hole (represented by the open circle) prefers to reside on one sublattice. This hole is on the “wrong” sublattice (with high energy cost) in the intermediate state above, which only acts as a technical tool for effectively generating the same sublattice hopping in the low energy limit. The constraint in Eq. (2.8) is obeyed on all sites in all the states shown.

written as

$$\mathcal{H}_{qd} = \mathcal{H}_d + \mathcal{H}_h + \mathcal{H}_t \quad (2.1)$$

The first term, \mathcal{H}_d involves a diagonal energy and a resonance of dimers on a plaquette, as illustrated in Fig 1a. Following Ref. 7, and the notation of Ref. 8, the dimers are represented by the conjugate phase $\hat{\mathcal{A}}_{i\alpha}$ and integer number $\hat{E}_{i\alpha}$ variables which reside on the links of the lattice:

$$[\hat{\mathcal{A}}_{i\alpha}, \hat{E}_{j\beta}] = i\delta_{ij}\delta_{\alpha\beta}. \quad (2.2)$$

The dimer number on a bond is $\eta_i \hat{E}_{i\alpha}$ oriented to the right or the top ($\eta_i = +1$ or -1 on the two sublattices). The Hamiltonian for dimers on a plaquette is

$$\mathcal{H}_d = \frac{V}{2} \sum_{i\alpha} \hat{E}_{i\alpha}^2 + J \sum_i \cos\left(\epsilon_{\alpha\beta} \Delta_\alpha \hat{\mathcal{A}}_{i\beta}\right) \quad (2.3)$$

Note that the co-efficient of the cosine has the “wrong” sign. This is a consequence of the microscopics of the electrons in the t - J model, if one adopts the natural sign convention that a singlet dimer is created by an electron pair-field operator (see Eq. (3.6)), and a given dimer covering corresponds to a product of such operators acting on the vacuum.

The next two terms, \mathcal{H}_h and \mathcal{H}_t , describe the hopping of holes in the doped dimer model, as illustrated in Fig 1b. To maintain the description in terms of nearest neighbor dimers, the holes must hop between sites on the same sublattice. Consequently, the model has two species of holes, one for each sublattice. This same-sublattice hole hopping model is somewhat inconvenient to work with under the duality mapping, and so we expand the Hilbert space of the model by additional high energy states to allow us to express all hole motion in

terms of nearest neighbor hopping: we allow each hole species to temporarily hop onto the “wrong” sublattice in a state which has a large energy. This hole will quickly hop back onto the “right” sublattice, and the two hop process will have achieved the same sublattice hopping we are seeking to model. This process is illustrated in Fig 1b; the same strategy was used by Moessner *et al.*¹⁸ in their study of the doped dimer model. We represent the two species of holes by the rotor phases $\hat{\phi}_{i+}$, $\hat{\phi}_{i-}$ and the conjugate number variables \hat{n}_{i+} , \hat{n}_{i-} . The commutation relations are

$$[\hat{\phi}_{i\sigma}, \hat{n}_{j\sigma'}] = i\delta_{ij}\delta_{\sigma\sigma'} \quad (2.4)$$

where $\sigma = +, -$. These holes reside primarily on the $+$ or $-$ sublattices and will have opposite gauge charges. The potential energy of the holes is described by \mathcal{H}_h :

$$\mathcal{H}_h = \frac{U}{2} \sum_{i\sigma} (\hat{n}_{i\sigma} - H - \sigma\eta_i W)^2 + \sum_{i \neq j, \sigma} \Lambda_{ij} \hat{n}_{i\sigma} \hat{n}_{j\sigma}. \quad (2.5)$$

Here $U > 0$ is the hole self repulsion, $2H$ is the average hole density preferred by the chemical potential (we are working at fixed chemical potential, and the actual density, δ , in the ground state of the Hamiltonian may be different), $\eta_i = \pm 1$ on the two sublattices, and $2UW$ is the energy penalty for a hole to be on the “wrong” sublattice. For $W > 0$, the $+$ holes are preferred on the $\eta_i = 1$ sublattice, and the $-$ holes on the other. The off-site interaction energy Λ_{ij} is assumed to be repulsive, and is required to stabilize insulating states away from zero doping. We will discuss the case of general Λ_{ij} , although our numerical results later will be restricted to short-range Λ_{ij} ; long-range Coulomb interactions lead only to minor modifications. The total density of holes on site i is given by

$$\delta_i = \sum_{\sigma} \langle \hat{n}_{i\sigma} \rangle. \quad (2.6)$$

The nearest neighbor hopping Hamiltonian for the two hole species is

$$\mathcal{H}_t = -t \sum_{i\alpha\sigma} \cos\left(\Delta_\alpha \hat{\phi}_{i\sigma} + \sigma \hat{\mathcal{A}}_{i\alpha}\right). \quad (2.7)$$

Finally, there is a local constraint, which commutes with all the terms in the Hamiltonian,

$$\Delta_\alpha \hat{E}_{i\alpha} + \sum_{\sigma} \sigma \hat{n}_{i\sigma} = \eta_i. \quad (2.8)$$

This constraint ensures that there is either a hole on each lattice site or a dimer emerging from it. It also allows for a configuration with two dimers emerging from that site if the extra gauge charge is compensated by an additional hole from the “wrong” sublattice. This is the intermediate state in Fig 1b which compared with the other two states in that figure requires the excitation energy $V/2 + UW$. We see that for sufficiently large V

we can safely set W equal to zero and still pay a price for having a hole on the “wrong” sublattice. Choosing both V and U sufficiently large also excludes unphysical states with even larger excitation energies. Note that all the states in Fig 1 obey Eq. (2.8).

We have already noted that the dimer resonance term in Eq. (2.3) has the opposite sign from that usually found for the Maxwell term in lattice gauge theories. We will see below that this can have significant consequences for the physics, and hence the structure of the dual theory. Physically, the kinetic term in Eq. (2.3) favors an average π flux per plaquette in the gauge field $\hat{A}_{i\alpha}$. The hole propagation term, Eq. (2.7), however, clearly allows holes to achieve lower kinetic energy if this flux is expelled. Since the gauge field is dynamical, the system will choose for itself what flux penetrates each plaquette on average, based on a balance of these two competing energies, and as pointed out by Kivelson and Fradkin⁷, the flux will penetrate at $\delta = 0$ and be expelled for large enough δ . In a strongly confining phase, as occurs for $\delta = 0$, however, this flux has no physical significance, since the gauge field is strongly fluctuating.

Mathematically, one may choose to view either the zero or π flux states as vacua, provided fluctuations of this flux are included. In particular, one may attempt to fix the sign “problem” ($J > 0$) by shifting the gauge field $\hat{A}_{i\alpha}$ on certain links by π . However, this has the effect of inducing a π flux per plaquette in the motion of the $\phi_{i\sigma}$ holes in Eq. (2.7). If we were to perform such a transformation, \mathcal{H}_d and \mathcal{H}_t would be replaced by

$$\mathcal{H}'_d = \frac{V}{2} \sum_i \hat{E}_{i\alpha}^2 - J \sum_i \cos(\epsilon_{\alpha\beta} \Delta_\alpha \hat{A}_{i\beta}), \quad (2.9)$$

$$\mathcal{H}'_t = -t \sum_{i\alpha\sigma} \cos(\Delta_\alpha \hat{\phi}_{i\sigma} + \sigma \hat{A}_{i\alpha} + 2\pi g_{i\alpha}), \quad (2.10)$$

and the holes now move in a magnetic field $g_{i\mu}$ which obeys

$$\epsilon_{\mu\nu\lambda} \Delta_\nu g_{i\lambda} = h \delta_{\mu\tau} \quad (2.11)$$

with $h = 1/2$.

For (most of) our purposes, it will generally not be advantageous to make such a shift. This is physically because our description of the Mott transition approaches the critical point from the superconducting side, in terms of the condensation of vortices of the superconducting state. As discussed above, in the large δ region of the dimer model where superconductivity occurs, zero flux is favored. Hence this is a more natural point from which to embark upon our (dual) investigation.

In the following section, however, in which we discuss quasiparticle physics and pairing symmetry, we will consider the physical content of this π -flux background. Our intuition to expand around the zero flux configuration is there confirmed, as we show that the π -flux background is inconsistent with d -wave (or s -wave) pairing in the superconductor, and applies instead to a yet more unconventional state.

III. ADDING FERMIONS AND SPIN TO THE DIMER MODEL

In the context of the cuprates, a shortcoming of the present approach – intrinsic to the dimer model – is the neglect of fermionic spin-carrying quasiparticles. To understand the nature of this difficulty more deeply, we discuss the results of a natural extension of the dimer approach to include these $S = 1/2$ fermionic excitations. The dimer model can also be extended to include collective $S = 1$ ‘triplon’ excitations, but we defer discussion of these to Section V, until after we have performed a duality analysis of the $S = 0$ dimer model in Section IV.

Readers mainly interested in the duality analysis of the $S = 0$ dimer model at finite doping may skip ahead to Section IV, and return to the present section upon a second reading.

The strategy will be to first understand in more detail the nature of the insulating states of this model when *undoped*. Because in this model at half-filling all the “matter” (holes and fermions) is gapped, the Polyakov argument implies that the U(1) gauge theory must be in a confining phase. Nevertheless, it is instructive to consider formally the limit of weak gauge fluctuations, which in practice applies for large J – of either sign. Then one may view the insulator as a gapped U(1) state plus gauge fluctuations, the latter – more specifically monopole proliferation – ultimately leading to confinement on long length scales, and with it, density wave order. This view has the advantage that the superconducting state can be seen as a “Higgs” phase obtained from the U(1) state. Further, the insulator can be characterized by a PSG, defining the manner in which the physical symmetries are realized in the gauge theory. Here we will consider two such PSGs, which correspond naturally to the phases obtained for large positive and negative J .

We can better understand in this manner the nature of the superconducting and insulating states in this model. We will see that the former should be understood as a “molecular” or “strong pairing” d -wave phase. The latter can be seen to arise from either of two natural underlying U(1) spin liquid states. These two U(1) states are distinct, and characterized by different PSGs. They are, however, both unstable at low energies to the various charge ordered states discussed herein.

We proceed with a multi-pronged attack. First, we describe the symmetry of the bosonic dimer+hole Hamiltonian of Sec. II. We consider the two distinct cases in which the ground state has an average zero or π gauge flux per plaquette. These two cases give rise to distinct PSGs which describe different putative insulating states. With this in hand, we discuss the nature of the pairing symmetry of superconducting states obtained from this model. Next, we will augment the dimer+hole Hilbert space by allowing each site to contain an unpaired electron (or spin), in addition to the end of a dimer or the hole allowed up to now. Physical arguments give the general form of the Hamiltonian with such unpaired electrons

included. This form is further restricted by combining the PSGs of the dimer+hole model and the requirement that physical electrons transform properly. We discuss how this analysis is related to slave particle formulations of Mott insulating states and Wen's analysis¹⁶ of their PSGs. With the full form of the dimer+hole+electron Hamiltonian determined, we confirm the symmetry analysis of the superconducting states by a direct investigation of the effective Bogoliubov-deGennes quasiparticle Hamiltonian.

A. Projectively realized symmetries of the doped dimer model

It is clear that, even without including fermionic excitations, the dimer model in Sec. II already requires a non-trivial projective realization of certain symmetry operations of the space group. This is so because the staggered static gauge charges (and the staggered potential term W in Eq. (2.5)) naïvely break lattice symmetries. To overcome this, unit translations and $\pi/2$ rotations about a dual lattice site must be accompanied by the transformations $\hat{n}_+ \leftrightarrow \hat{n}_-$, $\hat{\phi}_+ \leftrightarrow \hat{\phi}_-$, $\hat{A} \rightarrow -\hat{A}$, $\hat{E} \rightarrow -\hat{E}$ to leave the dimer model invariant. Actually, it will prove useful to discuss projective symmetries with respect to a fixed average background U(1) flux. This will make contact with Wen's notion of projective symmetry analysis of slave particle saddle points. We will consider the two cases of zero and π average flux per plaquette.

For compactness, we will in this section denote the boson operators by

$$b_{i\sigma} = e^{-i\hat{\phi}_{i\sigma}}. \quad (3.1)$$

Further, it is sometimes helpful to take the limit $W \rightarrow \infty$, corresponding to a "microscopic" dimer+hole model in which two holes of course cannot occupy the same site. In this case the type 1 holes live only on the A sublattice, and conversely the type 2 holes live only on the opposite B sublattice. One then defines a single boson field via

$$b_i = \begin{cases} e^{-i\hat{\phi}_{i+}} & \text{for } i \in A \text{ sublattice} \\ e^{-i\hat{\phi}_{i-}} & \text{for } i \in B \text{ sublattice} \end{cases}, \quad (3.2)$$

i.e. $b_i = b_{i\sigma}$ if i is on the σ sublattice. For $W \rightarrow \infty$, all finite energy states can be described in terms of the b_i operator. For $W < \infty$, this is not the case, but b_i defined as above is still useful and represents properly the low energy hole degrees of freedom.

1. Zero flux background

First, and simplest, is the case of zero flux, the naïve choice for $J < 0$ (note that which saddle point is chosen by the system is however a dynamical question, which will in general depend upon all the degrees of freedom,

and may vary as other parameters in the Hamiltonian are varied). In this case, one can easily see that the only non-trivial *required* aspect of transformations of the bosons is the interchange of the two boson flavors – and associated change of the sign of gauge fields – for space group operations that interchange the two sublattices. Specifically, these are unit translations (or generally translations by an odd number of total lattice units), $\pi/2$ rotations about a dual lattice site, and inversions through a row/column of the dual lattice. However, there is a mathematical freedom to compose each space group operation with a global U(1) phase rotation. That is, for an operation which preserves the two sublattices, one may take a priori

$$b_{i\sigma} \rightarrow b_{G(i)\sigma} e^{i\chi(G)}. \quad (3.3)$$

Similarly, for an operation that interchanges the two sublattices,

$$b_{i\sigma} \rightarrow b_{G(i),-\sigma} e^{i\chi(G)}. \quad (3.4)$$

Using the definition Eq. (3.2), both these equations are replaced simply by

$$b_i \rightarrow b_{G(i)} e^{i\chi(G)}. \quad (3.5)$$

Here $G(i)$ is the site i is mapped to under the space group operation G , and $\chi(G)$ is the phase, which we take as *the same* for both boson flavors, and can be chosen differently for each G . Note that this phase rotation is not a U(1) gauge rotation (which would be opposite for the two boson flavors) unless $e^{i\chi(G)} = \pm 1$. Since the hole fields are not themselves physical, it is not a priori obvious which value of $\chi(G)$ is the *correct* one.

An important constraint on $\chi(G)$ is that any sequence of space group operations which compose to the trivial identity operation in the original space group should compose to a pure gauge U(1) transformation in the PSG. The square of an inversion or the fourth power of a $\pi/2$ rotation must be a pure U(1) gauge transformation. Hence the phase $e^{4i\chi(I)} = 1$ if I is an inversion, while $e^{8i\chi(R)} = 1$ if R is a $\pi/2$ rotation. Other similar constraints can be applied with more detailed considerations.

For the doped dimer model, we can further refine this by using the physical interpretation of the hole operators. Consider the action of the physical singlet pair field operator on a bond:

$$\Psi_{i\alpha} = c_{i,s}^\dagger \epsilon_{ss'} c_{i+\hat{e}_\alpha, s'}, \quad (3.6)$$

with $\alpha = x, y$. Clearly, this operator, when acting on a state in which the bond in consideration is occupied by two holes, annihilates the holes and creates a dimer. Hence we require

$$\Psi_{i\alpha} = \mu_\alpha b_i b_{i+\hat{e}_\alpha} e^{i\eta_i \hat{A}_{i\alpha}}. \quad (3.7)$$

Here we have introduced two unknown coefficients, μ_x, μ_y (these are assumed independent of i , as can be argued is

generally true). To determine them, we use the known transformation properties of the pair field defined from Eq. (3.6). First, it is invariant under inversion through the row/column of the dual lattice dividing the two sites of the pair. This implies $e^{2i\chi(I)} = 1$ (actually this is true for all inversions). Then $e^{i\chi(I)} = \pm 1$, and for such values the phase rotation in Eq. (3.4) is a gauge U(1) rotation. Thus we can always choose

$$e^{i\chi(I)} = 1. \quad (3.8)$$

Second, consider a $\pi/2$ rotation. Under rotation around site i , Eq. (3.6) implies $\Psi_{ix} \rightarrow \Psi_{iy}$, $\Psi_{iy} \rightarrow \Psi_{i-\hat{e}_x,x}$, while from Eq. (3.7), one finds

$$\Psi_{ix} \rightarrow e^{2i\chi(R)} \frac{\mu_x}{\mu_y} \Psi_{iy}, \quad (3.9)$$

$$\Psi_{iy} \rightarrow e^{2i\chi(R)} \frac{\mu_y}{\mu_x} \Psi_{i-\hat{e}_x,x}. \quad (3.10)$$

Hence

$$e^{2i\chi(R)} = \frac{\mu_x}{\mu_y} = \pm 1. \quad (3.11)$$

No further requirements on $\chi(R)$ and μ_α follow from symmetry alone. The two choices in Eq. (3.11) simply represent different possible PSGs. Note that this choice is directly related to the pairing symmetry of the superconducting state. If $\mu_x = \mu_y$, then a uniform condensate $\langle b_i \rangle = \text{constant}$ represent an s -wave paired state, while for $\mu_x = -\mu_y$, the same condensate represents $d_{x^2-y^2}$ -wave pairing. More generally, using Eq. (3.7), one can show

$$\frac{\Psi_{iy} \Psi_{i+\hat{e}_x,y}}{\Psi_{ix} \Psi_{i+\hat{e}_y,x}} = \left(\frac{\mu_y}{\mu_x} \right)^2 e^{-i\eta_i \epsilon_{\alpha\beta} \Delta_\alpha \hat{A}_{i\beta}}, \quad (3.12)$$

where the curl in the exponential on the right hand side is the gauge flux through the plaquette with site i at the lower-left corner. Hence for the zero background flux states we consider in this subsection, using Eq. (3.11), one sees that

$$\frac{\Psi_{iy} \Psi_{i+\hat{e}_x,y}}{\Psi_{ix} \Psi_{i+\hat{e}_y,x}} = 1. \quad (3.13)$$

This allows for both s and d -wave pairing.

2. π flux background

Let us now turn to the more complicated case in which half a quantum of background gauge flux pierces each plaquette of the direct lattice. We write

$$\hat{A}_{i\alpha} \rightarrow \bar{A}_{i\alpha} + \hat{A}_{i\alpha}, \quad (3.14)$$

where $\bar{A}_{i\alpha}$ is a classical c-number background vector potential representing π flux per plaquette. An extremely convenient and symmetrical choice for this section is

$$\bar{A}_{ix} = -\bar{A}_{iy} = \frac{\pi}{4} \eta_i. \quad (3.15)$$

One can readily see that, with this choice, the Hamiltonian remains invariant under the same translational operations as for zero background flux, i.e. for a unit translation,

$$\hat{T}_\alpha : \quad b_{i,\sigma} \rightarrow b_{i+\hat{e}_\alpha,\sigma}, \quad (3.16)$$

and $\hat{A}_{i\beta} \rightarrow -\hat{A}_{i+\hat{e}_\alpha,\beta}$ etc. Rotations about dual lattice sites, and inversions are also unchanged. Rotations around direct lattice sites are, however, non-trivial. For a $\pi/2$ rotation about a direct lattice site, one requires

$$b_{i1} \rightarrow e^{i\chi(R)} \zeta_i b_{R(i)1}, \quad (3.17)$$

$$b_{i2} \rightarrow e^{i\chi(R)} \zeta_i^* b_{R(i)2}, \quad (3.18)$$

where

$$\zeta_i = \begin{cases} 1 & \text{for } (i_x, i_y) = (0, 0) \pmod{2}, \\ -i & \text{for } (i_x, i_y) = (1, 0) \pmod{2}, \\ -1 & \text{for } (i_x, i_y) = (1, 1) \pmod{2}, \\ i & \text{for } (i_x, i_y) = (0, 1) \pmod{2}. \end{cases} \quad (3.19)$$

Note that, since ζ_i is real on the A sublattice, one has simply

$$b_i \rightarrow e^{i\chi(R)} \zeta_i^* b_{R(i)}. \quad (3.20)$$

We can now repeat the symmetry analysis done above for zero background flux. As before, assuming the form of Eq. (3.7), since the transformation law for inversions has not changed, one still obtains Eq. (3.8). Under rotations, however, one obtains the conditions

$$e^{2i\chi(R)} = -i \frac{\mu_x}{\mu_y} = \pm 1. \quad (3.21)$$

Note the important factor of i in Eq. (3.21) compared to Eq. (3.11). This implies very different pairing states if the bosons condensed in the π flux background. For instance, if the holons condense uniformly, $\langle b_i \rangle = \text{const.}$, then $\Psi_{iy} = \mp i \Psi_{ix} = \text{const.}$. This is incompatible with either d - or s -wave pairing, and indeed with rotational invariance (in a d -wave superconductor, rotational symmetry is unbroken for gauge-invariant observables).

One way to see this is to consider the ratio in Eq (3.12), which becomes in this case

$$\frac{\Psi_{iy} \Psi_{i+\hat{e}_x,y}}{\Psi_{ix} \Psi_{i+\hat{e}_y,x}} = -1, \quad (3.22)$$

irrespective of the spatial pattern of boson condensation. In more conventional terms, the superconducting states with holons condensed in the π -flux background have a pair wavefunction of $(1 \pm i)s_{x^2+y^2} + (1 \mp i)d_{x^2-y^2}$ form. Again it is clear that such a complex linear combination of extended s - and d -wave pairing breaks fourfold rotational symmetry.

B. Fermions

Having understood the possible PSGs of the dimer+boson model, we are prepared to discuss fermionic excitations. In principle, there are many distinct ways in which the fermions might transform consistent with the above PSGs. There is, however, clearly a physically preferred and simple choice. We proceed by allowing a site to be occupied not only by a hole and an end of a dimer, but also by an unpaired electron. This enlargement of the Hilbert space is represented by a spin-1/2 fermion mode on each site, described by canonical fermion creation/annihilation operators f_{is}^\dagger, f_{is} (s is a spin-1/2 index). The original model is to be viewed as the fermion vacuum. Clearly, the electron annihilation operator may act on a site with such an unpaired electron to create a hole and remove the fermion. Hence we require

$$c_{is} \sim b_i^\dagger f_{is} + \dots \quad (3.23)$$

the ellipses are included to emphasize that of course microscopically the electron annihilation operator can create other states. For instance, it may act upon a site which is part of a dimer to annihilate the dimer, create a hole on the site acted upon and create a fermion on the other site shared by the dimer; such terms would be of the form

$$c_{is} \sim \dots b_i^\dagger e^{i\hat{A}_{i\alpha}} \epsilon_{ss'} f_{i+\hat{e}_\alpha, s'}^\dagger + \dots \quad (3.24)$$

Such additional terms are of quantitative importance in analyzing a microscopic dimer+hole+fermion model. In any case, all such terms are such that the constraint in Eq. (2.8) is now expanded to

$$\Delta_\alpha \hat{E}_{i\alpha} + \sum_\sigma \sigma \hat{n}_{i\sigma} + \eta_i \sum_s f_{is}^\dagger f_{is} = \eta_i. \quad (3.25)$$

This constraint makes it clear that the f_{is} fermions carry staggered U(1) gauge charge.

The single term in Eq. (3.23), however, suffices to determine the transformation properties of the f_{is} operators, from the requirement that the physical electron operator c_{is} is a scalar. First, we see that the f_{is} fermion carries a staggered gauge charge of opposite sign on the two sublattices. Next, we note that with zero background flux, b_i is a scalar apart from the $\chi(G)$ factor discussed in the previous section. Hence

$$f_{is} \rightarrow e^{i\chi(G)} f_{G(i)s}, \quad \text{for zero background flux.} \quad (3.26)$$

With the π flux background, Eq. (3.26) holds for transformations other than the $\pi/2$ rotation about a direct lattice site. For this, one has

$$f_{is} \rightarrow e^{i\chi(R)} \zeta_i^* f_{R(i)s}, \quad \text{for } \pi \text{ background flux.} \quad (3.27)$$

At this point we note that the similarity between Eq. (3.23) and the means of introducing slave particle ‘‘holon’’ and ‘‘spinon’’ operators in the U(1) mean field

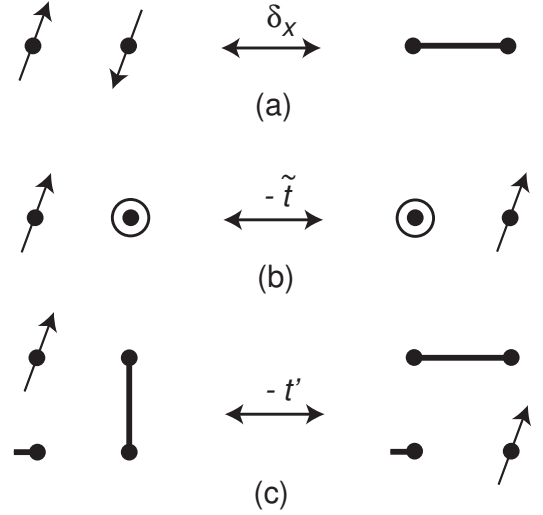


FIG. 2: Extension of Fig 1 to include $S = 1/2$ excitations in the dimer model. (a) Two $S = 1/2$ fermions forming a singlet valence bond, representing Eq. (3.28). (b) A holon and a $S = 1/2$ fermion exchanging positions, representing the first term in Eq. (3.30). (c) Motion of a $S = 1/2$ fermion involving rearrangement of valence bonds, representing the second term in Eq. (3.30).

theory of the $t - J$ model is not coincidental. Indeed, the universal aspects of this discussion can all be recovered as appropriate saddle points of that approach. They can also be recovered from the SU(2) mean field theory, the two approaches being interchangeable in this instance, as will be returned to below.

Having discussed the transformation properties of the fermions, we proceed to construct their Hamiltonian – assuming initially zero background field. Physically, the simplest allowed process is one in which a dimer converts to a singlet fermion pair (see Fig 2):

$$\mathcal{H}_f^{(1)} = v \sum_i f_{is}^\dagger f_{is} \quad (3.28) \\ + \sum_{i\alpha} \delta_\alpha e^{-i\eta_i \hat{A}_{i\alpha}} f_{is}^\dagger \epsilon_{ss'} f_{i+\hat{e}_\alpha, s'}^\dagger + \text{H.c.}$$

Here v represents the energy cost to introduce a single fermion, and the sums over the repeated spin indices s, s' are implicit. Taking $v \rightarrow \infty$ recovers the original dimer model. The coefficients δ_x, δ_y appear as ‘‘pair fields’’ for the f_{is} fermions. They are constrained by symmetry to satisfy

$$\delta_y = e^{-2i\chi(R)} \delta_x = \pm \delta_x, \quad \text{for zero background flux.} \quad (3.29)$$

We would also like to allow for hopping processes for the fermions. A fermion can hop between neighboring sites by exchanging places with a hole, or a fermion can hop between second neighbor sites if an intermediate neighboring site is connected to the destination site by a dimer, the dimer reconnecting after the hop to the origin

site. These processes are represented by

$$\begin{aligned} \mathcal{H}_f^{(2)} = & - \sum_{i\alpha} \tilde{t} b_i^\dagger b_{i+\hat{e}_\alpha} f_{i+\hat{e}_\alpha, s}^\dagger f_{i s} + \text{H.c.} \\ & - \sum_i t' \left[f_{i s}^\dagger f_{i+w, s} \Gamma_{i, i+w} + f_{i s}^\dagger f_{i+\bar{w}, s} \Gamma_{i, i+\bar{w}} + \text{H.c.} \right] \end{aligned} \quad (3.30)$$

where

$$\begin{aligned} \Gamma_{i, i+w} &= e^{-i\eta_i(\hat{A}_{ix} + \hat{A}_{i+\hat{e}_x, y})} + e^{-i\eta_i(\hat{A}_{iy} + \hat{A}_{i+\hat{e}_y, x})} \\ \Gamma_{i, i+\bar{w}} &= e^{-i\eta_i(\hat{A}_{ix} - \hat{A}_{i+\bar{w}, y})} + e^{-i\eta_i(\hat{A}_{i-\hat{e}_y, x} - \hat{A}_{i-\hat{e}_y, y})}, \end{aligned} \quad (3.31)$$

and $w = \hat{e}_x + \hat{e}_y$, $\bar{w} = \hat{e}_x - \hat{e}_y$. The complicated-looking Γ factors are simply the uniform superposition of the gauge connections (exponential of the discrete line integral of the gauge field) taken along the two shortest paths connecting diagonal sites. The equal superposition of both paths is required to preserve inversion symmetry through the (11) and (1 $\bar{1}$) axes of the square lattice. We give these t' terms primarily for completeness, as they will not have an important role in much of what follows.

By examination of Eqs. (3.28), (3.30), one sees that the $f_{i s}$ fermions hop unassisted (i.e. without accompanying holes) only between sites of the same sublattice, and experience pair fields on links connecting sites of opposite sublattices. This is indeed required by the staggered gauge charge of the $f_{i s}$ variables. It is thus sometimes convenient to define new variables via a particle-hole transformation:

$$d_{i s} = \begin{cases} f_{i s} & \text{for } \eta_i = +1, \\ \epsilon_{ss'} f_{i s'}^\dagger & \text{for } \eta_i = -1 \end{cases} \quad (3.32)$$

These $d_{i s}$ variables have a constant unit gauge charge on every site and transform as global SU(2) spinors. They should thus be identified as ‘‘spinons’’. In these variables, one finds that the constraint in Eq. (3.25) now takes the form

$$\Delta_\alpha \hat{E}_{i\alpha} + b_{i+}^\dagger b_{i+} - b_{i-}^\dagger b_{i-} + \sum_s d_{i s}^\dagger d_{i s} = 1, \quad (3.33)$$

while the Hamiltonian $\mathcal{H}_f = \mathcal{H}_f^{(1)} + \mathcal{H}_f^{(2)}$ has the form

$$\begin{aligned} \mathcal{H}_f = & v \sum_i \eta_i d_{i s}^\dagger d_{i s} + \sum_{i\alpha} t_{i\alpha} e^{-i\hat{A}_{i\alpha}} d_{i s}^\dagger d_{i+\hat{e}_\alpha, s} + \text{H.c.} \\ & + \tilde{t} \left[\sum_{i \in A, \alpha} b_{i+\hat{x}_\alpha}^\dagger b_i d_{i s}^\dagger \epsilon_{ss'} d_{i+\hat{x}_\alpha, s'}^\dagger \right. \\ & \left. + \sum_{i \in B, \alpha} b_i^\dagger b_{i+\hat{x}_\alpha} d_{i s}^\dagger \epsilon_{ss'} d_{i+\hat{x}_\alpha, s'}^\dagger + \text{H.c.} \right], \end{aligned} \quad (3.34)$$

and we have dropped the t' terms for brevity. Here the pairing terms for the $f_{i s}$ fermions have become hopping amplitudes:

$$t_{i\alpha} = \begin{cases} \delta_{i\alpha} & \text{for } \eta_i = +1, \\ -\delta_{i\alpha}^* & \text{for } \eta_i = -1. \end{cases} \quad (3.35)$$

From Eq. (3.34) one can clearly see that, if no holes are present (or if the b_i excitations are gapped), then the \tilde{t} term can be neglected, and the spinons $d_{i s}$ obey a simple tight-binding model. They indeed carry unit gauge charge, since they are minimally coupled to $\hat{A}_{i\alpha}$. We expect that the confining effects of \hat{A} fluctuations will produce VBS order in the insulator, and also bind the spinons into pairs which result in collective $S = 0$ and $S = 1$ excitations. Alternatively, the spinons can also confine with holons to create charged $S = 1/2$ excitations with the same quantum numbers as an electron.

In contrast, in the superconducting state (see Section III D below) the b_i are condensed, and then \mathcal{H}_f has the structure of the Bogoliubov theory of a superconductor, with the $d_{i s}$ acting as the $S = 1/2$ Bogoliubov quasiparticles; the b_i condensate also acts like a Higgs field which quenches the \hat{A} fluctuations. Indeed, if the b_i condensate is strong enough, there is nothing in Eq. (3.34) which prevents the appearance of gapless, nodal, Bogoliubov quasiparticles in a d -wave superconducting state (see also Section III D). In a superconductor which preserves all lattice symmetries, the nodal quasiparticles will appear above a critical doping $\delta = \delta_f$ as a quartet near the center of the Brillouin zone in a strong-pairing to weak-pairing transition¹⁹. On the other hand, the superconductor could also have broken lattice symmetries (i.e. it is a supersolid) and then the transition at $\delta = \delta_f$ is associated with the pairwise collision of nodal points at the reduced Brillouin zone boundaries^{13,14,20}.

Finally, it is useful to rewrite the expression for the physical electron field, Eq. (3.23), in the spinon variables:

$$c_{i s} \sim \begin{cases} b_i^\dagger d_{i s} & \text{for } \eta_i = +1, \\ -b_i^\dagger \epsilon_{ss'} d_{i s'}^\dagger & \text{for } \eta_i = -1 \end{cases} \quad (3.36)$$

At low energies, or in the $W \rightarrow \infty$ limit, this can be rewritten as

$$c_{i s} \sim b_{i+}^\dagger d_{i s} - b_{i-}^\dagger \epsilon_{ss'} d_{i s'}^\dagger, \quad (3.37)$$

since the first and second terms contribute predominantly on the A and B sublattices, due to the preferred locations of the two hole species.

How does this change for the π flux background? The needed form is obtained simply from Eqs. (3.28)-(3.34) by shifting according to Eq. (3.14). One notes that the $d_{i s}$ spinons, being minimally coupled to the gauge field, indeed propagate in this case according to a π -flux hopping model. Specifically, the shift implies

$$\delta_x \rightarrow \delta_x^{(\pi)} = \delta_x e^{-i\pi/4}, \quad (3.38)$$

$$\delta_y \rightarrow \delta_y^{(\pi)} = \delta_y e^{+i\pi/4}, \quad (3.39)$$

whence

$$t_{ix} \rightarrow t_{ix}^{(\pi)} = \eta_i \delta_x e^{-i\eta_i \pi/4}, \quad (3.40)$$

$$t_{iy} \rightarrow t_{iy}^{(\pi)} = \eta_i \delta_x e^{-2i\chi(R)} e^{+i\eta_i \pi/4}, \quad (3.41)$$

for real δ_x . Further, it is interesting to note in this case that the t' terms in Eq. (3.30) vanish with the replacement $\hat{A}_{i\alpha} = \bar{A}_{i\alpha}$ due to destructive interference of the

two hopping paths around the plaquette containing the two diagonal sites in question. Indeed, one can show from symmetry arguments alone that a diagonal hopping term is inconsistent with the π -flux PSG, using Eq. (3.27) for rotations and Eq. (3.26) for inversions.

C. Connection to slave particle theories

We comment briefly on the connection of the above discussion to the U(1) and SU(2) slave particle approaches to the $t-J$ model. The dimer model Hamiltonian above can be regarded as a theory of fluctuations around particular mean-field states of these approaches. This potentially allows one to connect to other gauge-theoretic scenarios and phases which are not within the purview of the dimer model. First consider the U(1) approach.^{9,10} One introduces microscopically holon and spinon fields via

$$c_{is} = b_i^\dagger f_{is}, \quad (3.42)$$

with the constraint $b_i^\dagger b_i + f_{is}^\dagger f_{is} = 1$. Eq. (3.42) should be compared with Eq. (3.23). Note that here there is only a single species of holon on each site, so we must compare directly to the dimer model in the large W limit. In the path integral Lagrangian, this constraint is implemented by a Lagrange multiplier A_{i0} :

$$\mathcal{L}_0 = - \sum_i iA_{i0}(b_i^\dagger b_i + f_{is}^\dagger f_{is} - 1). \quad (3.43)$$

The electron hopping (t) and Heisenberg (J) terms of the $t-J$ model are decoupled with matrix fields $Q_{ij}, \bar{Q}_{ij}, \Delta_{ij}$ leading to quadratic terms in the bosons and fermions of the form

$$\mathcal{L}_1 = \sum_{ij} \left(Q_{ij} b_i^\dagger b_j + \bar{Q}_{ij} f_{is}^\dagger f_{js} + \Delta_{ij} f_{is}^\dagger \epsilon_{ss'} f_{js'} + \text{H.c.} \right) \quad (3.44)$$

Comparison with the effective Hamiltonians in the dimer+hole+fermion model (for large W) above shows that one can obtain the same form at the quadratic level by taking a saddle point with $iA_{i0} = v\eta_i$, Q_{ij}, \bar{Q}_{ij} non-zero only when i, j are on the same sublattice, and $\Delta_{ij}, \bar{\Delta}_{ij}$ non-zero only when i, j are on opposite sublattices. For the π -flux case, Q_{ij}, \bar{Q}_{ij} actually are non-zero only between sites separated by an even number of lattice spacings in the x and y directions (corresponding to the vanishing of the t' couplings with this background, and hence to a four-sublattice structure of the bosons). Phase fluctuations of these matrix fields become the spatial components of the gauge fields of the dimer+hole+fermion model.

Next, consider the SU(2) slave particle formulation.^{11,12} In this case, one represents the electrons by an SU(2) doublet of bosons, $b_{i\sigma}$, and a

spin-1/2 fermion d_{is} , with the electron represented as

$$c_{is} = \frac{1}{\sqrt{2}} \left(b_{i+}^\dagger d_{is} + b_{i-}^\dagger \epsilon_{ss'} d_{is'}^\dagger \right). \quad (3.45)$$

Up to a sign change in b_{i-} (due to our trivially different conventions), this is the same form as Eq. (3.37). The slave particles are constrained by $\psi_{is}^\dagger \frac{\vec{\tau}}{2} \psi_{is} + b_i^\dagger \vec{\tau} b_i = 0$, where the doublet

$$\psi_{is} = \begin{pmatrix} d_{is} \\ \epsilon_{ss'} d_{is'}^\dagger \end{pmatrix}, \quad (3.46)$$

and $\vec{\tau}$ is the vector of Pauli matrices acting in the doublet space. These constraints lead to three Lagrange multipliers A_{i0}^p ($p = 1, 2, 3$):

$$\mathcal{L}_0^{SU(2)} = - \sum_{ip} i\vec{A}_{i0} \cdot \left(\psi_{is}^\dagger \frac{\vec{\tau}}{2} \psi_{is} + b_i^\dagger \vec{\tau} b_i \right). \quad (3.47)$$

Of particular interest is the $p = 3$ component of this constraint which takes the form

$$b_{i+}^\dagger b_{i+} - b_{i-}^\dagger b_{i-} + \sum_s d_{is}^\dagger d_{is} = 1. \quad (3.48)$$

Comparing Eq. (3.48) with our Eqs. (3.25), (3.33), we see that they differ in that Eqs. (3.25), (3.33) contain an additional fluctuating electric field contribution. This is a reflection of the different manner in which the gauge fluctuations are realized on the lattice, rather than a fundamental distinction. If we begin with a theory with a constraint as in Eq. (3.48), and imagine integrating out some high energy degrees of freedom, then the gauge invariance permits the electric field contribution in Eqs. (3.25), (3.33) to appear in the renormalized theory; thus, the main difference is that in our dimer model approach this contribution is already included in the bare theory.

As we will see in Section IV, in our duality analysis the electric field term is a large contribution to the l.h.s. of Eq. (3.25), which dominates that of the f fermions. In contrast, in the mean-field saddle points of Refs. 11,12, the dominant contribution to Eq. (3.48) arises from the fermion $d_{is}^\dagger d_{is}$ term, with the d fermions occupying a half-filled band (the d fermions also contribute a large term to the duality analysis of Section IV in Eq. (3.33), but not in a manifestly translationally invariant manner.²¹) We will comment further on the physical distinction between these two approaches in Section IV. Decoupling the hopping and Heisenberg interactions in the Hamiltonian gives quadratic terms for the slave particles of the form:

$$\mathcal{L}_1^{SU(2)} = \sum_{ij} c_1 \psi_{is}^\dagger U_{ij} \psi_{js} + c_2 b_i^\dagger U_{ij} b_j, \quad (3.49)$$

with

$$U_{ij} = \begin{pmatrix} -\chi_{ij}^* & \Delta_{ij} \\ \Delta_{ij}^* & \chi_{ij} \end{pmatrix}. \quad (3.50)$$

Our dimer+hole+fermion model described by $\mathcal{H}_{qd} + \mathcal{H}_f$ in Eqs. (2.1), (3.34) can be described in the above SU(2) formulation by taking a saddle point with $-iA_{i0}^3 = v\eta_i$. In particular, our physical interpretation requires that we take the saddle point value $-v \sim W$ large so that the $b_{i\sigma}$ holes reside primarily on their respective sublattices. In contrast, in previous work^{11,12} on the SU(2) gauge theory superficially different saddle points were chosen: they worked with a spatially uniform value of $-iA_{i0}^3$ so that only one species of the bosons was preferentially occupied in the ground state. However, saddle points in these two classes can be mapped onto each other by a SU(2) gauge transformation generated by the unitary matrix $i\tau^1$ acting only on the $\eta_i = -1$ sublattice. This gauge transformation maps our staggered $-iA_{i0}^3$ saddle point to a spatially uniform saddle point. The same gauge transformation acting on $\mathcal{L}_1^{SU(2)}$ interchanges the fermion hopping, χ_{ij} , and pairing, Δ_{ij} , terms. So to obtain a saddle point of $\mathcal{L}_1^{SU(2)}$ consistent with our Eq. (3.34) we need to take the Δ_{ij} of a form consistent with the $t_{i\alpha}$ in Eq. (3.34). The χ_{ij} will be proportional to the \hat{t} times the square of the b_i condensate.

When the model is undoped and the holons are gapped, $\langle b_i \rangle = 0$, such states fit into Wen's PSG classification scheme for symmetric spin liquid states on the square lattice. What are called the zero and π flux states in this paper correspond, in the notation of Ref. 16, to the states U1Cn00x, and U1Cn0n1, respectively (see Eqs (122) and (135) of Ref. 16). These states are distinct in their PSGs from the "staggered flux" and "pi flux" states of Refs. 11,12, which are denoted U1Cn01n and SU2Bn0, respectively in Ref. 16. Note that in Wen's discussion, the spin liquids U1Cn00x, and U1Cn0n1 obey the constraint in Eq. (3.48); consequently the fermion "chemical potential" v in Eq. (3.28) or Eq. (3.34) is not an arbitrary parameter and must take a value that ensures that Eq. (3.48) is obeyed. In our discussion, we have the additional fluctuating electric field contribution in Eq. (3.33), and we treat Eqns. (3.28) and (3.34) as generic effective Hamiltonians; large positive values of v , which lead to a large spin gap and a small density of f fermions, are also allowed.

D. Superconducting state

To obtain superconducting states of the doped (or undoped) dimer model, one clearly must condense some charged particle. In fact, a conventional superconducting state requires a condensation of both flavors of bosons, $\langle b_{i\sigma} \rangle \neq 0$ for both $\sigma = \pm$. Condensation of only one of the flavors breaks only the combination of physical U(1) charge symmetry (since each holon carries charge $+e$) and gauge U(1) symmetry. The orthogonal linear combination is unbroken in that case. Explicitly, one can see this from Eq. (3.37) and Eq. (3.34). When only one boson is condensed, say $\langle b_{i+} \rangle \neq 0$, then at mean-field level, the electron and spinon become equivalent, in this case

$c_{is} \sim \langle b_{i+} \rangle d_{is}$. Replacing d_{is} by c_{is} in Eq. (3.34) and dropping the \hat{t} term which vanishes since one of the two bosons is uncondensed, one sees that one has no anomalous electron pairing terms. One might also imagine condensing not the individual holon fields but instead just the quadratic forms $\langle b_{i+}^\dagger b_{j-} \rangle \neq 0$ and $\langle b_{i+}^\dagger b_{j-}^\dagger \rangle \neq 0$. This will certainly break the charge U(1) symmetry, and indeed follows if we condensed both holons individually. However, if the individual holons remain uncondensed, there is a residual unbroken Z_2 gauge symmetry under $b_{i\sigma} \rightarrow z_i b_{i\sigma}$, with $z_i = \pm 1$. Thus such a state is an anomalous superconductor (SC*), which we do not wish to consider here.

It is simplest to think about the "conventional" superconducting state in the b_i and f_{is} variables. Condensation of both flavors of holon then simply means that $\langle b_i \rangle$ is non-zero on both sublattices. Then, from Eq. (3.23), we can regard the f_{is} variables as essentially electrons. Formally, if the superconducting state does not break translational symmetry, the holon condensate will have uniform amplitude,

$$\langle b_i \rangle = |b| e^{-i\phi_i}, \quad (3.51)$$

so we shift $f_{is} \rightarrow e^{-i\phi_i} f_{is}$, after which $c_{is} \sim |b| f_{is}$. This gives

$$\begin{aligned} \mathcal{H}_f^{(1)} \rightarrow & v \sum_i f_{is}^\dagger f_{is} \\ & + \sum_{i\alpha} \delta_\alpha e^{i(\phi_i + \phi_{i+\hat{\epsilon}_\alpha})} f_{is}^\dagger \epsilon_{ss'} f_{i+\hat{x}_\alpha, s'}^\dagger + \text{H.c.}, \end{aligned} \quad (3.52)$$

where we have dropped the gauge field which is gapped by the Higgs mechanism in this phase. The rescaled fermion f_{is} can now be regarded as the electron quasiparticle operator, so that the pairing state can be read directly off from Eq. (3.52). We see that the pair amplitude obeys

$$\Psi_{i\alpha}^* \sim \delta_\alpha e^{i(\phi_i + \phi_{i+\hat{\epsilon}_\alpha})}. \quad (3.53)$$

This is in full agreement with the symmetry discussion in Sec. III A.

Note that for the case of a zero flux background, the pairing can be of $d_{x^2-y^2}$ symmetry. This occurs e.g. for a uniform holon condensate $\phi_i = 0$ and $\delta_x = -\delta_y = 1$ ($e^{2i\chi(R)} = -1$), or for $\phi_i = \pi i_x$ and $\delta_x = \delta_y = 1$ ($e^{2i\chi(R)} = 1$). Nevertheless, the spectrum of \mathcal{H}_f is fully gapped in the limit relevant to the doped dimer model, since there $v \gg \delta_\alpha$. This corresponds to a "molecular", "BEC", or "strong pairing" d-wave phase, where it is well-known that gapless nodal excitations are absent.

It is amusing to consider the energetics behind the pairing symmetry for one example. Let us take for simplicity zero background flux, and choose the PSG with $\delta_x = \delta_y$, $e^{2i\chi(R)} = 1$. To apply Eq. (3.53), we need to understand the pattern of holon condensation. For simplicity, let us ignore explicit (non-gauge mediated) holon-spinon interactions, and gauge fluctuations. Then we may consider the holons on their own, described by a hopping model.

We imagine lowering the chemical potential for holons until they condense, the condensate being built out of the lowest energy modes. Consider a single holon excitation. For simplicity, we consider the large W limit, so that the flavor 1 holons prefer to sit on the A sublattice and the other flavor sits on the B sublattice. For $W = \infty$, the lowest one-holon states are degenerate, consisting of any superposition of one holon of type 1 on the A sublattice, or any superposition of one holon of type 2 on the B sublattice. One can then apply degenerate perturbation theory to the holon hopping terms, to arrive at an effective model of the type 1 holon hopping on the A checkerboard sublattice and the type 2 holon hopping on the B checkerboard sublattice. One expects that, allowing for generalized hoppings in the original model, this hopping Hamiltonian takes the form

$$\mathcal{H}_{1h} = t_{\text{eff}} \sum'_{\langle ij \rangle} b_{i\sigma}^\dagger b_{j\sigma} + \dots, \quad (3.54)$$

where the prime on the sum indicates that the sum is over nearest neighbors of the A(B) sublattice for $\sigma = 1$ ($\sigma = 2$). The ellipses indicate other further neighbor terms that will generally be present. The single-holon eigenstates of Eq. (3.54) are plane waves, with energy $E_\sigma(k) = 2t_{\text{eff}}(\cos(k_x + k_y) + \cos(k_x - k_y))$ (momenta are defined for the original square lattice). For $t_{\text{eff}} < 0$, the minimum energy states have either $k_x = k_y = 0, \pi$. These two are actually equivalent, and represent states with constant b_i on the A or B sublattice. For $t_{\text{eff}} > 0$, the minimum energy states have $k_x = 0, k_y = \pi$ or $k_x = \pi, k_y = 0$, which are also equivalent and represent states with b_i alternating in sign on nearest-neighbor site of the A or B sublattice, e.g. with $b_{i+} = 1$ on sites with x_i, y_i both even and $b_{i-} = -1$ on sites with x_i, y_i both odd. At the one particle level, one expects then the condensate which forms on doping to be a linear superposition of these two flavors,

$$\langle b_i \rangle = \psi_1 b_{i+}^{\text{min}} + \psi_2 b_{i-}^{\text{min}}, \quad (3.55)$$

where $b_{i\sigma}^{\text{min}}$ is the minimum energy single-holon wavefunction with support only on the σ sublattice, either constant or staggered on this sublattice depending upon the sign of t_{eff} . The nature of the superposition that occurs – i.e. the coefficients ψ_1, ψ_2 – will be determined by holon-holon interactions. At a mean-field level, we can simply construct a “Landau” effective action for ψ_1, ψ_2 . Since both flavors of bosons are separately conserved, it should have $U(1) \times U(1)$ symmetry under rotations of each field. Further, it should be symmetric under interchange of the two flavors, by translation invariance, which interchanges the two sublattices. One expects therefore an effective (Euclidean) Lagrangian of the form

$$\mathcal{L}_{\text{eff}} = -r(|\psi_1|^2 + |\psi_2|^2) + u(|\psi_1|^2 + |\psi_2|^2)^2 - v|\psi_1|^2|\psi_2|^2. \quad (3.56)$$

The nature of the condensate depends upon the sign of v . For $v > 0$, one obtains $|\psi_1| = |\psi_2|$, while for $v < 0$,

one or the other amplitude vanishes. Since the latter case clearly breaks translational symmetry, we focus on the former. Then for $t_{\text{eff}} < 0$, the phases ϕ_i are constant on all sites of one sublattice, which for $t_{\text{eff}} > 0$, the ϕ_i alternate between 0 and π on the neighboring (diagonal second neighbors on the original square lattice) sites of a given sublattice.

Now let us consider the pairing symmetry. As we assumed $\delta_y = \delta_x$, we have from Eq. (3.53)

$$\frac{\Psi_{iy}}{\Psi_{ix}} = e^{i(\phi_{i+\hat{x}} - \phi_{i+\hat{y}})}. \quad (3.57)$$

Since $i + \hat{x}, i + \hat{y}$ are nearest neighbor sites on the same sublattice, one finds

$$\frac{\Psi_{iy}}{\Psi_{ix}} = \begin{cases} 1 & \text{for } t_{\text{eff}} < 0, \\ -1 & \text{for } t_{\text{eff}} > 0 \end{cases} \quad (3.58)$$

Thus the pairing is s -wave or d -wave in these two cases, respectively.

IV. DUALITY ANALYSIS OF THE DOPED DIMER MODEL

This section returns to an analysis the of effective theory of the total spin $S = 0$ sector presented in Section II. For this limited theory, we claim that the following analysis properly accounts for the strong fluctuations of the compact $U(1)$ gauge field \hat{A} ; a corresponding, non-perturbative treatment of gauge fluctuations has not so far been possible in the slave particle theories.^{10,11,12,13,14,15,16} The $S = 1/2$ fermions f_{is} are neglected below,²¹ and it is clear that this is surely safe as long as the f_{is} remain fully gapped. We noted in Section III B that the structure of our theory allows the appearance of gapless nodal fermionic excitations in the superconducting phases, and that they do not significantly modify the structure of the resulting superconductor. As long as such nodal excitations are present only for a $\delta > \delta_f$ for which the ground state is a superconductor or a supersolid, the following analysis will apply for the full range of δ . However, it is also possible that δ_f coincides with the position of a superconductor-insulator transition: such a critical point will not be described by the theories presented below and in I.

Before embarking upon our duality analysis, we remark further on why the neglect of the f_{is} fermions is not as dangerous as it might naively seem, and why it is amply compensated by the non-perturbative treatment of gauge fluctuations. It is useful to refer back to our key constraint equations Eq. (3.25), (3.33), and the corresponding constraint equation for the slave particle theory in Eq. (3.48). In the earlier slave particle theories, the dominant, order unity, and translationally invariant contribution to the l.h.s. of Eq. (3.48) is provided by the fermion density term $d_{is}^\dagger d_{is}$. However, by focusing on a static gauge field saddle point, these theories do not allow

a significant contribution to this constraint equation from the $\Delta_\alpha \hat{E}_{i\alpha}$ term on the l.h.s. of Eqs. (3.25), (3.33) (such contributions are only generated upon including fluctuations about the static gauge saddle points). In our duality approach below (and in the previous work^{3,7,8} on the undoped model) a large contribution is given by the $\Delta_\alpha \hat{E}_{i\alpha}$ term: this is only possible because we account for strong gauge fluctuations. The contribution of the f fermionic term in Eq. (3.25), from either nodal or gapped excitations, is small (note, however, that the contribution of the d fermion term in our Eq. (3.33) is *not* small²¹), and its neglect appears safe. Physically speaking, the $\Delta_\alpha \hat{E}_{i\alpha}$ term counts the valence bonds on the links emerging from a site, and so our approach here assumes that most of the electrons appear in singlet pairs, rather than individually in single particle states.

We proceed with a duality mapping of \mathcal{H}_{qd} as in Ref. 8 and similar to that described in I. The cosine term in \mathcal{H}_t is written in the Villain form as

$$\begin{aligned} & \exp\left(t\Delta\tau \cos\left(\Delta_\alpha \hat{\phi}_{i\sigma} + \sigma \hat{\mathcal{A}}_{i\alpha}\right)\right) \\ \rightarrow & \sum_{\{J_{i\sigma\alpha}\}} \exp\left(-\frac{J_{i\sigma\alpha}^2}{2t\Delta\tau} + iJ_{i\sigma\alpha}\Delta_\alpha \hat{\phi}_{i\sigma} + i\sigma J_{i\sigma\alpha}\hat{\mathcal{A}}_{i\alpha}\right), \end{aligned} \quad (4.1)$$

while that in \mathcal{H}_d is written as

$$\begin{aligned} & \exp\left(-J\Delta\tau \cos\left(\epsilon_{\alpha\beta}\Delta_\alpha \hat{\mathcal{A}}_{i\beta}\right)\right) \rightarrow \\ & \sum_{\{B_a\}} \exp\left(-\frac{B_a^2}{2J\Delta\tau} + iB_a\epsilon_{\alpha\beta}\Delta_\alpha \hat{\mathcal{A}}_{i\beta} + i\pi B_a\right). \end{aligned} \quad (4.2)$$

Here B_a is an integer-valued dual magnetic field on the sites of the dual lattice. Then we integrate over the $\phi_{i\sigma}$ and $\mathcal{A}_{i\alpha}$ and obtain the dual partition function

$$\begin{aligned} \mathcal{Z}_{qd} = & \sum_{\{J_{i\sigma\mu}, F_{a\mu}\}} \exp\left(-\frac{g}{2} \sum_a F_{a\mu}^2 - i\pi \sum_a F_{a\tau}\right. \\ & - \frac{1}{2e^2} \sum_{i\sigma} [J_{i\sigma\mu} - (H + \sigma\eta_i W)\delta_{\mu\tau}]^2 \\ & - \Delta\tau \sum_{i \neq j, \sigma} \Lambda_{ij} J_{i\sigma\tau} J_{j\sigma\tau} \left. \right) \prod_{i\sigma} \delta(\Delta_\mu J_{i\sigma\mu}) \\ & \times \prod_{a\mu} \delta\left(\epsilon_{\mu\nu\lambda}\Delta_\nu F_{a\lambda} + \sum_\sigma \sigma J_{i\sigma\mu} - \eta_i \delta_{\mu\tau}\right) \end{aligned} \quad (4.3)$$

where $J_{i\sigma\mu} = (n_\sigma, J_{i\sigma x}, J_{i\sigma y})$ represent the integer valued spacetime currents of the two species of holes, $F_{a\mu} = (-B_a, -E_{iy}, E_{ix})$ is the integer valued gauge flux, $g = 1/(J\Delta\tau) = V\Delta\tau$, and as in I, $e^2 = t\Delta\tau = 1/U\Delta\tau$. The $i\pi F_{a\tau}$ term will be innocuous in the present subsection, and we will return to a consideration of its effects in Section IV C when we examine the signature of the electronic pairing.

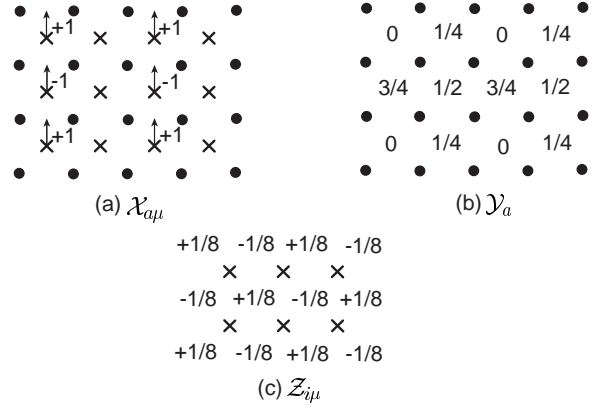


FIG. 3: The values of the only non-zero components of the fixed field $\mathcal{X}_{a\mu}$, \mathcal{Y}_a , and $\mathcal{Z}_{i\mu}$. The circles (crosses) are the sites of the direct (dual) lattice. In (c), only the $\mu = \tau$ component of $\mathcal{Z}_{i\mu}$ is non-zero and its values are shown.

We solve the constraints in Eq. (4.3) by parameterizing

$$\begin{aligned} J_{i\sigma\mu} &= \epsilon_{\mu\nu\lambda}\Delta_\nu b_{a\sigma\lambda} \\ F_{a\mu} &= \Delta_\mu N_a + \mathcal{X}_{a\mu} - \sum_\sigma \sigma b_{a\sigma\mu} \end{aligned} \quad (4.4)$$

The integer-valued fixed field $\mathcal{X}_{a\mu}$ is defined as in Ref. 8 and is shown in Fig 3; it obeys the constraint

$$\epsilon_{\mu\nu\lambda}\Delta_\nu \mathcal{X}_{a\lambda} = \eta_i \delta_{\mu\tau} \quad (4.5)$$

The degrees of freedom are integers $b_{a\sigma\mu}$ on the links of the dual lattice and integers N_a on the sites of the dual lattice.

Now we promote these integer-valued fields to real fields by introducing a vortex fugacity y_v and a monopole fugacity y_m . Then

$$\begin{aligned} \mathcal{Z}_{qd} = & \prod_{a\sigma} \int db_{a\sigma\mu} \int d\vartheta_{a\sigma} \int dN_a \exp\left[\right. \\ & - \frac{g}{2} \sum_a \left(\Delta_\mu N_a + \mathcal{X}_{a\mu} - \sum_\sigma \sigma b_{a\sigma\mu}\right)^2 \\ & - i\pi \sum_a \left(\Delta_\tau N_a + \mathcal{X}_{a\tau} - \sum_\sigma \sigma b_{a\sigma\tau}\right) \\ & - \frac{1}{2e^2} \sum_{i\sigma} [\epsilon_{\mu\nu\lambda}\Delta_\nu b_{a\sigma\lambda} - (H + \sigma\eta_i W)\delta_{\mu\tau}]^2 \\ & - \Delta\tau \sum_{a \neq a', \sigma} \Lambda_{ij} \epsilon_{\tau\nu\lambda}\Delta_\nu b_{a\sigma\lambda} \epsilon_{\tau\rho\varrho}\Delta_\rho b_{a'\sigma\varrho} \\ & + y_v \sum_{a\sigma} \cos(\Delta_\mu \vartheta_{a\sigma} - 2\pi b_{a\sigma\mu}) \\ & \left. + y_m \sum_a \cos\left(2\pi N_a - \sum_\sigma \sigma \vartheta_{a\sigma}\right)\right] \end{aligned} \quad (4.6)$$

This is a theory of 2 vortex fields, $\psi_+ = e^{i\vartheta_+}$ and $\psi_- = e^{i\vartheta_-}$ which are coupled to 2 non-compact U(1)

gauge fields $b_{+\mu}$ and $b_{-\mu}$. There is also a Higgs field N_a which breaks the staggered component of the U(1) gauge symmetries, as will become more explicit below.

We will henceforth not carry through the off-site Λ_{ij} terms explicitly in our analysis. As in I, we will assume that their effects can be absorbed into a renormalization of the value of e^2 . This is certainly the case for short-range Λ_{ij} , while for long-range Coulomb interactions, e^2 will acquire momentum dependence which was noted in I. Our numerical results below will be restricted to the short-range case, but we do not expect significant modifications for the long-range case.

To allow us to make direct contact with previous work on the undoped dimer model, we use the parameterization of $\mathcal{X}_{a\mu}$ in Ref. 8 in terms of curl-free and divergence-free fields (shown in Fig 3)

$$\mathcal{X}_{a\mu} = \Delta_\mu \mathcal{Y}_a + \epsilon_{\mu\nu\lambda} \Delta_\nu \mathcal{Z}_{i\lambda}. \quad (4.7)$$

Inserting this in Eq. (4.6) and shifting $N_a \rightarrow N_a - \mathcal{Y}_a$ we obtain

$$\begin{aligned} \mathcal{Z}_{qd} = & \prod_{a\sigma} \int db_{a\sigma\mu} \int d\vartheta_{a\sigma} \int dN_a \exp \left[\right. \\ & - \frac{g}{2} \sum_a \left(\Delta_\mu N_a + \mathcal{E}_{a\mu} - \sum_\sigma \sigma b_{a\sigma\mu} \right)^2 \\ & - i\pi \sum_a \left(\Delta_\tau N_a + \mathcal{E}_{a\tau} - \sum_\sigma \sigma b_{a\sigma\tau} \right) \\ & - \frac{1}{2e^2} \sum_{i\sigma} [\epsilon_{\mu\nu\lambda} \Delta_\nu b_{a\sigma\lambda} - (H + \sigma\eta_i W) \delta_{\mu\tau}]^2 \\ & + y_v \sum_{a\sigma} \cos(\Delta_\mu \vartheta_{a\sigma} - 2\pi b_{a\sigma\mu}) \\ & \left. + y_m \sum_a \cos \left(2\pi N_a - \sum_\sigma \sigma \vartheta_{a\sigma} - 2\pi \mathcal{Y}_a \right) \right], \quad (4.8) \end{aligned}$$

where $\mathcal{E}_{a\mu} = \epsilon_{\mu\nu\lambda} \Delta_\nu \mathcal{Z}_{i\lambda}$ is given by

$$\mathcal{E}_{a\mu} \equiv \frac{(-1)^{a_x + a_y}}{4} (0, 1, -1). \quad (4.9)$$

It is convenient to introduce uniform (A_μ) and ‘staggered’ (C_μ) gauge fields defined by

$$\begin{aligned} b_{a+\mu} &= A_{a\mu} + C_{a\mu} \\ b_{a-\mu} &= A_{a\mu} - C_{a\mu}. \end{aligned} \quad (4.10)$$

The term proportional to g in Eq. (4.8) effectively breaks the ‘staggered’ gauge symmetry associated with C_μ under which ψ_\pm have opposite gauge charges. The field N_a is the phase of the Higgs field which breaks this symmetry, and as is conventional, we use a gauge transformation to set this field equal to 0. Also, we transform from the hard-spin to soft-spin variables to obtain the dual action

in its final form

$$\begin{aligned} \mathcal{Z}_{qd} = & \prod_{a\mu} \int dA_{a\mu} \int dC_{a\mu} \prod_{a\sigma} \int d\psi_{a\sigma} \exp \left[\right. \\ & - \frac{1}{e^2} \sum_a [\epsilon_{\mu\nu\lambda} \Delta_\nu A_{a\lambda} - H \delta_{\mu\tau}]^2 \\ & - \frac{1}{e^2} \sum_i [\epsilon_{\mu\nu\lambda} \Delta_\nu C_{a\lambda} - \eta_i W \delta_{\mu\tau}]^2 \\ & - \frac{g}{2} \sum_a (2C_{a\mu} - \mathcal{E}_{a\mu})^2 + 2i\pi \sum_a C_{a\tau} \\ & - \sum_{a\sigma} \left[s |\psi_{a\sigma}|^2 + \frac{u}{2} |\psi_{a\sigma}|^4 \right] - v \sum_a |\psi_{a+}|^2 |\psi_{a-}|^2 \\ & + \frac{y_v}{2} \sum_{a\sigma\mu} \left[\psi_{a+\mu,\sigma}^* e^{2\pi i (A_{a\mu} + \sigma C_{a\mu})} \psi_{a\sigma} + \text{c.c.} \right] \\ & \left. + \frac{y_m}{2} \sum_a \left[\psi_{a-}^* \psi_{a+} e^{2\pi i \mathcal{Y}_a} + \text{c.c.} \right] \right]. \quad (4.11) \end{aligned}$$

The similarity between \mathcal{Z}_{qd} above, and the dual theory of bosons on a square lattice in I should now be evident. The latter theory had a single vortex species, ψ_a , coupled to a single non-compact U(1) gauge field $A_{a\mu}$. Here in Eq. (4.11) we have two vortex species, ψ_{a+} and ψ_{a-} , but they are coupled together by the monopole fugacity term proportional to y_m , effectively reducing the theory to that of a single vortex field. The present partition function also has 2 non-compact U(1) gauge fields, $A_{a\mu}$ and $C_{a\mu}$, but the $C_{a\mu}$ field has acquired a mass from the Higgs phenomenon, as is clear from the term proportional to g . This massive gauge field also has a complex Berry phase term (with $2i\pi$ in Eq. (4.11)), which is unimportant here because the $C_{a\mu}$ fluctuations are quenched. The physical meaning of this quenching was already discussed at the end of Sec. II: in this representation, the regime of interest where the dimer resonance move has relatively small amplitude corresponds to large g , and the π gauge flux favored by this term (responsible for the complex Berry phase term just mentioned) is expelled.

Given the close similarity between \mathcal{Z}_d in I and \mathcal{Z}_{qd} in Eq. (4.11), it is evident that low energy fluctuations in the vicinity of transitions between superfluid, supersolid, and insulating phases of the quantum dimer model are described by the *same* continuum quantum field theories as those in I. The most important fact determining the character of these field theories is the particular projective representation of the square lattice space group (PSG) that is realized by the saddle point under consideration. In particular, all we need is the value of the effective dual ‘magnetic’ flux f , and the corresponding value of the unimodular complex number ω in I. Determining this requires a careful symmetry analysis of the appropriate saddle point of Eq. (4.11), and this is carried out in the following subsection.

Before turning to this symmetry analysis, it is useful to make explicit contact between the dual partition function in Eq. (4.11), and previous dual representations^{3,8} of

the *undoped* dimer model. The hole density vanishes in this limit, and so the $A_{a\mu}$ flux is zero; this is achieved by setting $H = 0$ in Eq. (4.11). Furthermore, the insulating behavior requires a strong condensate of the $\psi_{a\pm}$ fields, and we can focus on the phase fluctuations of the condensate by writing $\psi_{a\pm} = e^{i\chi_{a\pm}}$. We also set the massive field $C_{a\mu} = 0$. Then the action \mathcal{Z}_{qd} maps at low energies to

$$\begin{aligned} \mathcal{Z}_{qd} = & \prod_{a\mu} \int dA_{a\mu} \prod_{a\sigma} \int d\chi_{a\sigma} \exp \left[\right. \\ & - \frac{1}{e^2} \sum_a [\epsilon_{\mu\nu\lambda} \Delta_\nu A_{a\lambda}]^2 \\ & - \frac{y_v}{2} \sum_{a\mu} \left(\frac{\Delta_\mu \chi_{a+} + \Delta_\mu \chi_{a-}}{2} + 2\pi A_{a\mu} \right)^2 \\ & - \frac{y_v}{8} \sum_{a\mu} (\Delta_\mu \chi_{a+} - \Delta_\mu \chi_{a-})^2 \\ & \left. + y_m \sum_a \cos(\chi_{a+} - \chi_{a-} + 2\pi \mathcal{Y}_a) \right]. \quad (4.12) \end{aligned}$$

The first two terms show that the A_μ gauge field is Higgsed by $\chi_{a+} + \chi_{a-}$, and so is innocuous. The last two terms constitute a sine-Gordon model for $\chi_{a+} - \chi_{a-}$, with on-site offset \mathcal{Y}_a : this is precisely the dual representation of the undoped dimer model found earlier^{3,8}.

A. Symmetries

As in I, we will analyze the symmetry properties of the dual dimer model theory in Eq. (4.11) at a commensurate density of holes appropriate to a proximate Mott insulator. We assume this has the rational value δ_I which we parameterize as

$$\frac{\delta_I}{2} = \frac{p}{q}, \quad (4.13)$$

where p and q are relatively prime integers. In general (as in I), the density of holes, δ , in the theory in Eq. (4.11) is determined by the parameter H , and in the superfluid or supersolid phases we may have $\delta \neq \delta_I$.

Proceeding as in I, we set the gauge field $A_{a\mu}$ equal to a saddle point value $\bar{A}_{a\mu}$ such that the flux is equal to the density of each species of hole (+ or -). So we choose $\bar{A}_{a\tau} = \bar{A}_{ax} = 0$ and

$$\bar{A}_{ay} = \frac{\delta_I}{2} a_x. \quad (4.14)$$

For the staggered gauge field we have the saddle point value $\bar{C}_{a\mu} = \frac{\lambda}{2} \mathcal{E}_{a\mu}$ with $\lambda = 1/(1 + 4/e^2 g)$.

The main new subtlety here (beyond that of I) in the symmetry analysis of Eq. (4.11) is the presence of the fixed background fields $\mathcal{E}_{a\mu}$ and \mathcal{Y}_a . These fields are not explicitly invariant under the square lattice space group,

and so require additional transformations of the vortex fields upon operations of the space group. These additional transformation will modify the needed PSG, as shown below.

Carrying out the space group operations in the presence of the $\bar{A}_{a\mu}$, $\mathcal{E}_{a\mu}$, and \mathcal{Y}_a , it can be shown that the action remains invariant under the following field transformations, which are the analog of the relations in Section II.B of I:

$$\begin{aligned} T_y & : \psi_+(k_x, k_y) \rightarrow \psi_-(k_x, k_y) e^{-ik_y} e^{i\pi/4} \\ T_y & : \psi_-(k_x, k_y) \rightarrow \psi_+(k_x, k_y) e^{-ik_y} e^{-i\pi/4} \\ T_x & : \psi_+(k_x, k_y) \rightarrow \psi_-(k_x, k_y - \pi\delta_I) e^{-ik_x} e^{-i\pi/4} \\ T_x & : \psi_-(k_x, k_y) \rightarrow \psi_+(k_x, k_y - \pi\delta_I) e^{-ik_x} e^{i\pi/4} \\ R_{\pi/2} & : \psi_+(k_x, k_y) \rightarrow \\ & \frac{1}{q} \sum_{m,n=0}^{q-1} \psi_-(k_y + \pi n\delta_I, -k_x + \pi m\delta_I) \omega^{-mn} \\ R_{\pi/2} & : \psi_-(k_x, k_y) \rightarrow \\ & \frac{1}{q} \sum_{m,n=0}^{q-1} \psi_+(k_y + \pi n\delta_I, -k_x + \pi m\delta_I) \omega^{-mn} \end{aligned} \quad (4.15)$$

To understand the degeneracy of the spectrum associated with these transformations, it is useful to transform to a basis of states which are eigenvectors of T_y . These are expressed by the fields

$$\begin{aligned} \psi_1 & = \frac{1}{\sqrt{2}} \left(e^{-i\pi/8} \psi_+ + e^{i\pi/8} \psi_- \right) \\ \psi_2 & = \frac{1}{\sqrt{2}} \left(e^{-i\pi/8} \psi_+ - e^{i\pi/8} \psi_- \right). \end{aligned} \quad (4.16)$$

Then

$$\begin{aligned} T_y & : \psi_1(k_x, k_y) \rightarrow \psi_1(k_x, k_y) e^{-ik_y} \\ T_y & : \psi_2(k_x, k_y) \rightarrow -\psi_2(k_x, k_y) e^{-ik_y} \\ T_x & : \psi_1(k_x, k_y) \rightarrow \psi_2(k_x, k_y - \pi\delta_I) e^{-ik_x} e^{i\pi/2} \\ T_x & : \psi_2(k_x, k_y) \rightarrow \psi_1(k_x, k_y - \pi\delta_I) e^{-ik_x} e^{-i\pi/2} \\ R & : \psi_1(k_x, k_y) \rightarrow \frac{1}{q} \sum_{m,n=0}^{q-1} \omega^{-mn} \\ & \quad \times \frac{[\psi_1 + i\psi_2](k_y + \pi n\delta_I, -k_x + \pi m\delta_I)}{\sqrt{2}} \\ R & : \psi_2(k_x, k_y) \rightarrow -\frac{1}{q} \sum_{m,n=0}^{q-1} \omega^{-mn} \\ & \quad \times \frac{[\psi_2 + i\psi_1](k_y + \pi n\delta_I, -k_x + \pi m\delta_I)}{\sqrt{2}}. \end{aligned} \quad (4.17)$$

Now we observe that the T_y eigenvalues of the ψ_1 fields at momentum k are equal to those of the ψ_2 fields at $k + (0, \pi)$. So these fields will mix with each other, and cannot lead to orthogonal eigenmodes. It is convenient to introduce a new collective field $\Psi(k)$ which equals ψ_1 at k

and ψ_2 at $k + (0, \pi)$, and which is identified by the eigenvalue e^{-ik_y} of T_y . Then, ignoring unimportant phase factors, we have under the action of T_x :

$$T_x : \Psi(k_x, k_y) \rightarrow \Psi(k_x, k_y + \pi - \pi\delta_I) \quad (4.18)$$

From this equation we see that the PSG of the present fields has the same structure as that in Section I of I

$$\begin{aligned} T_x T_y &= \omega T_y T_x, \\ \omega &\equiv e^{2\pi i f} \end{aligned} \quad (4.19)$$

with the key parameter f specified by

$$f \equiv \frac{\tilde{p}}{\tilde{q}} = \frac{(1 - \delta_I)}{2} = \frac{1}{2} - \frac{p}{q}, \quad (4.20)$$

where \tilde{p} and \tilde{q} are also relatively prime integers. Note that the value of f is half the density of *electrons* *i.e.* it is the density of Cooper pairs in the Mott insulator. So the low energy field theory of the present dimer model is identical to that presented in I but with the PSG determined by the density of Cooper pairs. We have also explicitly diagonalized the spectrum of $\psi_{a\sigma}$ vortices in \mathcal{Z}_{qd} in Eq. (4.11) and verified that it did indeed have the degeneracy required by such a PSG.

B. Mean field theory

We have seen above that the low energy continuum theory of the quantum dimer model is identical to that already presented in I. We have already presented a mean-field analysis of this continuum theory in Section II.D of I, and so do not need to repeat it here. Rather, we will work directly with the lattice action in Eq. (4.11) and follow its mean-field phase diagram with increasing hole density, δ .

To do a mean-field analysis of our dual dimer model we consider the free energy corresponding to Eq. (4.11). Rescaling the fields $\psi_{a\sigma}$, and neglecting an overall constant, we can choose $u = y_v = 1$ and obtain the free energy (with $r \equiv s - 2$)

$$\begin{aligned} \mathcal{F} &= \frac{1}{2} \sum_{a\sigma\mu} \left| \psi_{a+\mu,\sigma} e^{-2\pi i(A_{a\mu} + \sigma C_{a\mu})} - \psi_{a\sigma} \right|^2 \\ &+ \sum_{a\sigma} \left[r |\psi_{a\sigma}|^2 + \frac{1}{2} |\psi_{a\sigma}|^4 \right] + v \sum_a |\psi_{a+}|^2 |\psi_{a-}|^2 \\ &- \frac{y_m}{2} \sum_a [\psi_{a-}^* \psi_{a+} e^{2\pi i \mathcal{Y}_a} + \text{c.c.}] \\ &+ \frac{1}{e^2} \sum_a [\epsilon_{\mu\nu\lambda} \Delta_\nu A_{a\lambda} - H \delta_{\mu\tau}]^2 \\ &+ \frac{1}{e^2} \sum_a [\epsilon_{\mu\nu\lambda} \Delta_\nu C_{a\lambda} - \eta_{ia} W \delta_{\mu\tau}]^2 \\ &+ \frac{g}{2} \sum_a (2C_{a\mu} - \mathcal{E}_{a\mu})^2. \end{aligned} \quad (4.21)$$

For simplicity we will also set y_m equal to 1, and, as discussed below Eq. (2.8), we can safely choose $W = 0$. We will set v equal to zero and do not discuss states which break the $\sigma \rightarrow -\sigma$ symmetry. Such states break the vortex-anti-vortex symmetry on average, and emerge only for sufficiently large v .

We note that we have dropped the $2i\pi \sum_a C_{a\tau}$ term in Eq. (4.11), which was a consequence of the sign $J > 0$ in the dimer ‘resonance’ term Eq. (2.9). The massive $C_{a\tau}$ field has little effect on our analysis below, and it therefore appears reasonable to ignore this term in our mean-field theory.

This leaves us with the hole chemical potential (the ‘magnetic field’) H (in the superfluid phase, this picks a hole density $\delta = 2H$), the coupling constants e^2 and g , and the control parameter r . For the phase transition between the superfluid and the insulating phase to be of second order we have to choose e^2 small. In our units, we take $e^2 = 0.04$.

We can now map out the phase diagram for zero doping. Instead of using r and g as parameters, let us use r and the already introduced (below Eq. (4.14)) parameter

$$\lambda \equiv \frac{1}{1 + 4/e^2 g}. \quad (4.22)$$

Note that the range $0 < g < \infty$ gets mapped onto $0 < \lambda < 1$. Also, in the superfluid phase, and close to the second order phase transition to this phase, the saddle point approximation for the massive field $C_{a\mu}$ becomes exact such that $B_{\text{staggered}} = \epsilon_{\tau\mu\nu} \Delta_\mu C_{a\nu} = \pm\lambda/2$.

As can be seen in Fig 4, for large enough r we are always in the superfluid phase, which is characterized by the vortex vacuum $\langle \psi_{a\mu} \rangle = 0$. As we decrease r , we enter an insulating state with $\langle \psi_{a\mu} \rangle \neq 0$ via a second order phase transition. Depending on the value of λ , this can either be a columnar valence bond solid (VBS) state (B), or a state with site density wave order (CDW) at wavevector (π, π) (A). It turns out that the plaquette state (C) always has a free energy slightly larger than that of the columnar VBS state, for the parameters chosen here. All these results are consistent with the mean field phase diagram of our field theory for $q = 2$ in I.

In Fig 4 (and Figs 6-9) we have indicated the links of the direct lattice by solid lines. The size of the (black) bars living on these links is proportional to the vortex kinetic energy

$$\langle \psi_{a+\mu,\sigma}^* e^{2\pi i(A_{a\mu} + \sigma C_{a\mu})} \psi_{a\sigma} + \text{c.c.} \rangle, \quad (4.23)$$

which we can physically interpret as the mean spin exchange energy of the electrons on the direct lattice. The mean electron ring exchange energy determined by

$$\langle \psi_{a-}^* \psi_{a+} e^{2\pi i \mathcal{Y}_a} + \text{c.c.} \rangle \quad (4.24)$$

is depicted by (blue) boxes whose size is chosen to be proportional to this quantity. If the exchange energy is negative we have used a crossed box. Finally the (mean)

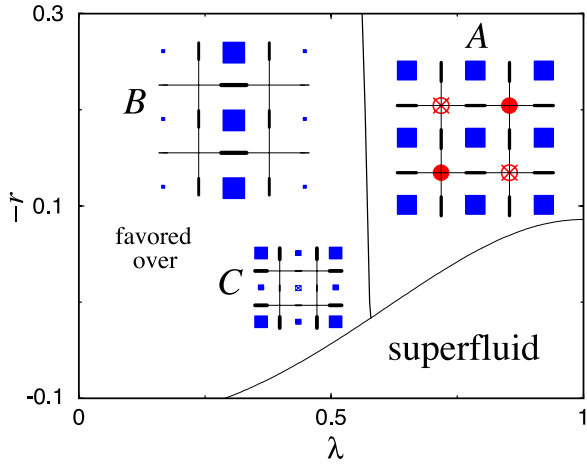


FIG. 4: Mean field phase diagram for the doped dimer model with zero doping. For large r our theory favors a vortex vacuum such that we are in the superfluid phase. Decreasing r we enter one of the (condensed) insulating states. While for smaller λ we find a columnar bond ordered state (B) whose free energy is slightly lower than that of a plaquette state (C), for larger values of λ we get a CDW state (A). The lines indicate the links of the direct lattice. The black bars on these links are proportional to the spin exchange energy or the electron pairing amplitude (see text). Similarly, the size of the (blue) boxes depicts the ring exchange amplitudes which are located on the dual lattice. If this amplitude is negative we have used a (tiny) crossed box. Finally, the state A also shows a finite mean hole density which is positive on one sublattice (red bullets) and negative on the other (crossed circles). As discussed in the text this CDW state is unphysical, and we exclude the corresponding parameter values.

density of holes on the sites of the direct lattice is proportional to

$$B_i \equiv \Delta_x A_{a_i y} - \Delta_y A_{a_i x}. \quad (4.25)$$

For $H = 0$ (zero doping) we expect this quantity to vanish, which indeed is the case for the bond ordered or the plaquette state. However, the CDW state in Fig 4 shows a checkerboard pattern for B_i , which takes opposite values on the two sublattices, and are depicted by (red) bullets or crossed circles depending on whether B_i is positive or negative. Clearly this CDW state is not in a physically interesting regime of couplings for the original dimer model as it applies to the cuprates (the electron density is uniform in the Mott insulator at half-filling); the lesson to be learned from this is that in our model we cannot choose g too large. For concreteness, let us choose $g = 2/e^2 = 50$ such that for sufficiently small r we are always in the columnar VBS state.

To discuss doping holes into an insulator, we will start from a columnar bond ordered state and follow its fate as we increase the chemical potential H . First of all, it is instructive to determine the critical value of r at which we have the phase transition from a superfluid to an insulating state as a function of H . This transition occurs when the $\psi_{a\mu}$ condense, and so a lower bound on the critical

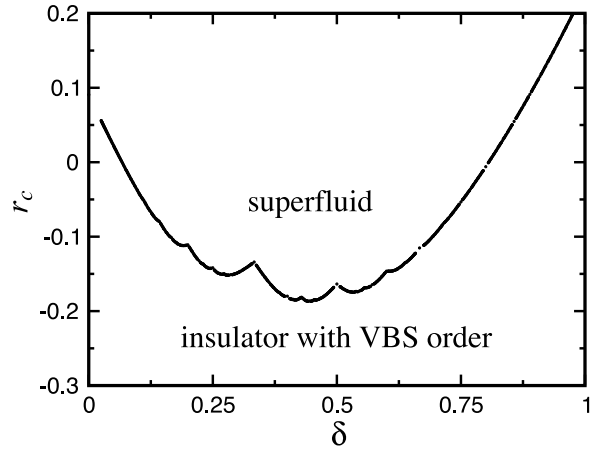


FIG. 5: Lower bound for the superfluid to insulator transition, r_c as a function of the hole density, δ , in the superfluid state ($\delta = 2H$). There is a second order transition at the points shown into an insulator with the same density. For irrational δ , this insulator is a floating Wigner solid. The rational δ Mott insulators are expected to survive in fixed density "Mott lobes" extending over a finite range of the "chemical potential" H , and these can pre-empt the transition into the incommensurate floating solids. The re-entrance of the curve above at large H is in a regime of such large δ that we do not expect our small doping theory to remain valid.

value of $r = r_c$ is obtained by locating the point at which the lowest eigenvalue of the quadratic part of the $\psi_{a\mu}$ free energy in Eq. (4.21) turns negative. A graph of the lower bound of $r_c(H)$ is shown in Fig 5. Determination of this lowest eigenvalue requires the Hofstadter spectrum of $\psi_{a\mu}$, and so the graph in Fig 5) has a shape similar to the ground state energy of the Hofstadter butterfly. For incommensurate values of H , the transition at the points in Fig 5 is into a floating Wigner solid with hole density $\delta = 2H$. We expect that this will often be pre-empted by a first order transition into a nearby commensurate Mott insulator with hole density $\delta \neq 2H$, but instead at the rational value determined by the Mott insulator. In the dual language of the 'superconductor', this Mott insulator has expelled some of the 'magnetic flux' H .

In the following we will choose $r = -0.1$ such that we are in the insulating state at zero doping, and enter the superfluid phase at around $\delta \approx 0.15$. Our mean field theory also predicts that at high enough doping concentration we are back in an insulating state, but we do not expect our duality analysis to be valid at such large δ .

We do not make any pretense at completeness in the following phase diagrams: they are merely representative structures obtained for a sample set of parameters, and other parameters can clearly give a wide variety of other phases. However, all such phases will obey the general constraints we have delineated in I.

In Figs. 6-9 we show the states for doping $\delta = 0, 1/32, 1/16$, and $1/8$. While at zero doping we are in a columnar VBS state with vanishing hole density on the sites, at doping $\delta = 1/32$ we find a modified plaquette

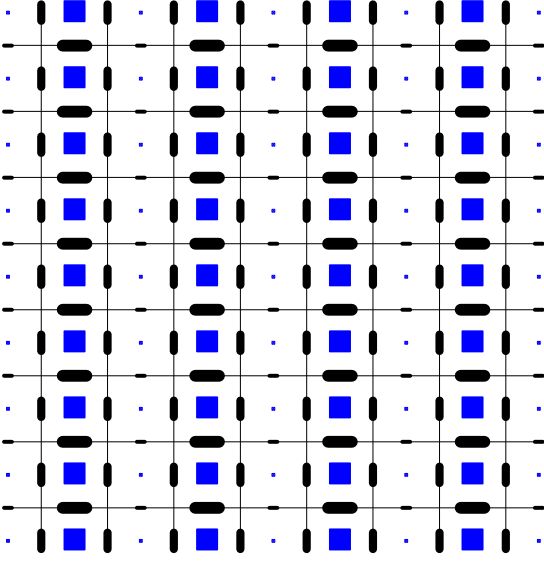


FIG. 6: Insulating state with columnar valence bond solid (VBS) order at zero doping. This state is obtained by a mean-field minimization of the free energy in Eq. (4.21) with parameter values as discussed in the text. The significance of the symbols on the square lattice above (and in Figs 7-9) are as in Fig 4.

state and which shows a concentration of the mean hole density at the corners of one plaquette of its 8×8 unit cell. At the center of this plaquette frustration leads to $\langle \psi_{a+} \rangle = \langle \psi_{a-} \rangle = 0$. The variation of charge density in the unit cell clearly results in a 2-dimensional charge density wave with wave-vectors $\mathbf{k}_x = (2\pi/8a, 0)$ and $\mathbf{k}_y = (0, 2\pi/8a)$ where a is the lattice spacing. It should also be noted that as for the plaquette state (C) in Fig 4, the state depicted in Fig 7 is invariant under rotations by 90 degrees about the plaquette with $\langle \psi_{a\sigma} \rangle = 0$.

Doubling the doping concentration δ , we find the state depicted in Fig 8, which is similar to the previous state but has a unit cell of half its size and leads to a modulation of the charge density with wave-vectors $\mathbf{k}_{\pm} = (2\pi/8a, \pm 2\pi/8a)$. Finally at doping $\delta = 1/8$, we find the state depicted in Fig 9 which is also invariant under rotations by 90 degrees about a plaquette with $\langle \psi_{a\sigma} \rangle = 0$ and has a 4×4 unit cell. Since we are now close to the second order phase transition to the superfluid phase, the mean hole density is now distributed essentially uniformly over the lattice. However, there is still a weak 2-dimensional hole density modulation with wave-vectors $\mathbf{k}_x = (2\pi/4a, 0)$ and $\mathbf{k}_y = (0, 2\pi/4a)$

C. Pairing symmetry

The analysis of this section has been carried out almost entirely in a dual representation of the underlying electronic degrees of freedom. While this has the benefit

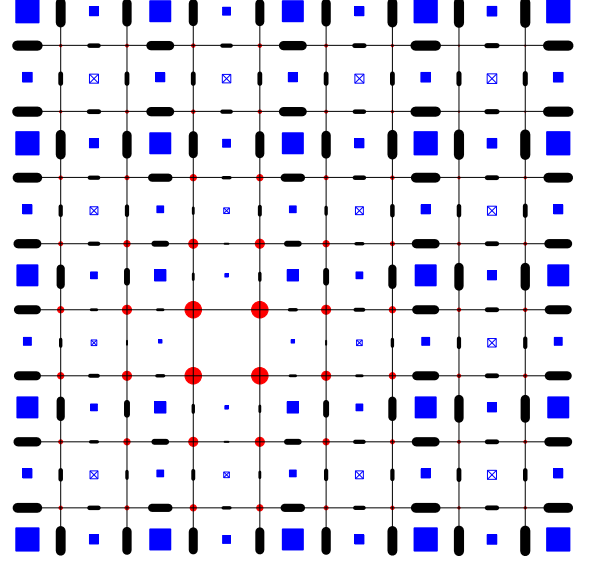


FIG. 7: An insulating state with a 8×8 unit cell for doping $\delta = 1/32$. The parameters are the same as for the $\delta = 0$ state in Fig 6, apart from the change in H , the hole chemical potential. This state is invariant under rotations by 90 degrees around the plaquette with $\langle \psi_{a\sigma} \rangle = 0$. The mean hole density indicated by the red bullets is concentrated near this plaquette.

of properly accounting for the non-perturbative dynamics of the compact $U(1)$ gauge theory \mathcal{H}_{qd} in Eq. (2.1), it does obscure the physical interpretation of the phases of the theory. We have already shown in I how the density wave order can be thoroughly characterized by the dual vortex degrees of freedom. In this subsection we want to determine and analyze the corresponding dual representation of correlators which characterize the superconducting order.

We already discussed the issue of the pairing symmetry in Section III A and found that certain key determining factors could not be specified within the physics of the dimer model alone. In Eq. (3.7) we related the electron pairing field to the product of microscopically determined co-efficients μ_{α} and degrees of freedom of the quantum dimer model. Let us consider the two-point correlation function for the pair field, at two pairs of nearest-neighbor points 12, 34, where 2 is displaced in direction α from 1, and 4 is displaced in direction β from 3 (see Fig 10 for an example). Then we can write the pairing correlator as

$$\langle \Psi_{12} \Psi_{34}^* \rangle = \mu_{\alpha} \mu_{\beta} G_{12;34} \quad (4.26)$$

where $G_{12;34}$ is a two-point correlator of the quantum dimer model given by

$$G_{12;34} = \langle C_{34}^{\dagger} C_{12} \rangle, \quad (4.27)$$

with the gauge-invariant hole pair annihilation operator

$$C_{12} = e^{i\eta_1 \hat{A}_{12}} e^{-i\hat{\phi}_{1+}} e^{-i\hat{\phi}_{2-}}. \quad (4.28)$$

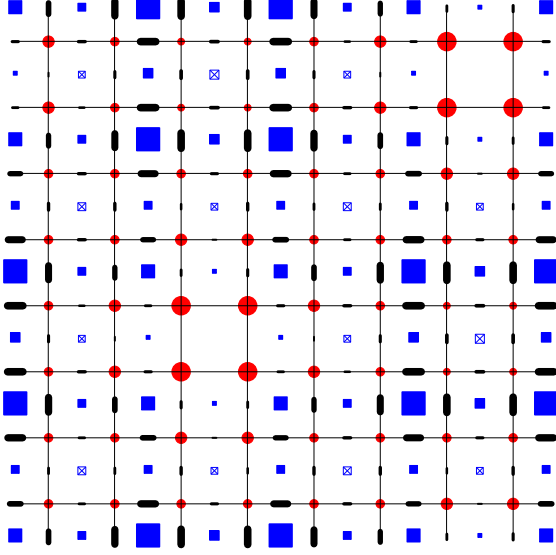


FIG. 8: Insulating state evolving out of state in Fig 7 for doping $\delta = 1/16$ (other parameters as in Fig 6). As for the state depicted in Fig 7 this state is symmetric under rotations by 90 degrees. However, the unit cell is now 4×8 .

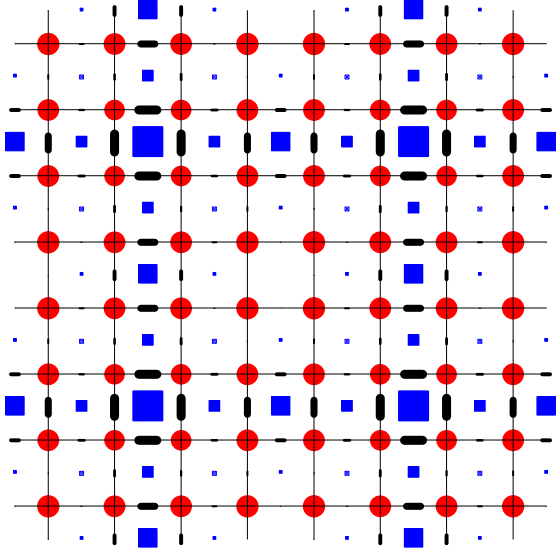


FIG. 9: Insulating state for doping $\delta = 1/8$ with a 4×4 unit cell, with parameters as in Figs. 6-8. Now we are close to the phase transition to the superfluid phase and the mean hole density is more evenly distributed.

We choose sites 1,3 on the A sublattice ($\eta_i = +1$) and sites 2,4 on the B sublattice ($\eta_i = -1$) for concreteness.

It now remains to evaluate $G_{12;34}$ within the context of duality analysis of Section IV. We will show that this correlator factorizes in the limit of large separation between the points 12 and 34, with no dependence on the rela-

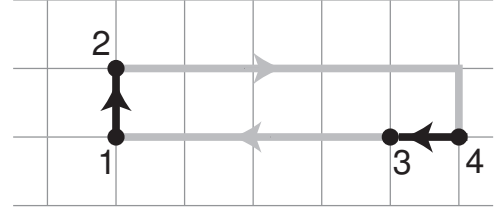


FIG. 10: Computation of the electron pair correlation function. The sites 1,3 have $\eta_i = +1$, while 2,4 have $\eta_i = -1$. The current $J_{31\mu}$ is equal to unity along the line connecting 3 to 1, and is zero elsewhere; other currents between two points are defined similarly. We also define *loop* currents *e.g.* $J_{1243\mu}$ is unity only along the loop around the points 1,2,4,3. An electron singlet pair is created on the link 1,2 and annihilated on the link 3,4.

tive orientations or centers of 12 and 34. This is indicative of superconducting Off-Diagonal Long Range Order (ODLRO). The symmetry of the pairing state is then determined by the dependence of $\langle \Psi_{12} \Psi_{34}^* \rangle$ on either pair of neighboring points 34 or 12, separately. Consequently the pairing symmetry of the superfluid ground state is determined by the μ_α factors controlling the particular PSG realized by the dimer model, *and* by the dependence of $G_{12;34}$ on 12 or 34 separately. We will see that, for the large g limit on which we focus, $G_{12;34}$ is also independence of the orientation or position of either pair of points when they are well-separated. Thus the pairing symmetry is determined *entirely* by the μ_α factors.

The correlator $G_{12;34}$ can be computed in our dual representation by inserting the operator in Eq. (4.28), and the corresponding operator at sites 3,4, into the transformations leading to Eq. (4.3). After integrating over the degrees of freedom on the direct lattice as before, the correlation function is expressed as

$$\begin{aligned}
 G_{12;34} = & \frac{1}{\mathcal{Z}_{qd}} \sum_{\{J_{i\sigma\mu}, F_{a\mu}\}} \exp \left(-\frac{g}{2} \sum_a F_{a\mu}^2 - i\pi \sum_a F_{a\tau} \right. \\
 & - \frac{1}{2e^2} \sum_i \left([J_{i+\mu} + J_{31\mu} - (H + \eta_i W)\delta_{\mu\tau}]^2 \right. \\
 & \left. \left. + [J_{i-\mu} - J_{24\mu} - (H - \eta_i W)\delta_{\mu\tau}]^2 \right) \right) \prod_{i\sigma} \delta(\Delta_\mu J_{i\sigma\mu}) \\
 & \times \prod_{a\mu} \delta \left(\epsilon_{\mu\nu\lambda} \Delta_\nu F_{a\lambda} + J_{1243\mu} + \sum_\sigma \sigma J_{i\sigma\mu} - \eta_i \delta_{\mu\tau} \right)
 \end{aligned} \tag{4.29}$$

Here the currents $J_{12\mu}$ etc. are fixed background currents defined in Fig 10 associated with the presence of the source terms of the correlator. Notice that the delta function constraints in Eq. (4.29) differ importantly from those in Eq. (4.3); consequently the solution of these con-

straints in Eq. (4.4) is replaced by

$$\begin{aligned} J_{i\sigma\mu} &= \epsilon_{\mu\nu\lambda}\Delta_\nu b_{a\sigma\lambda} \\ F_{a\mu} &= \Delta_\mu N_a + \mathcal{B}_{a\mu} + \mathcal{X}_{a\mu} - \sum_\sigma \sigma b_{a\sigma\mu}, \end{aligned} \quad (4.30)$$

where $\mathcal{B}_{a\mu}$ is a fixed background integer-valued field which obeys

$$\epsilon_{\mu\nu\lambda}\Delta_\nu \mathcal{B}_{a\lambda} = -J_{1243\mu}. \quad (4.31)$$

Therefore, $\mathcal{B}_{a\mu}$ is the ‘‘magnetic’’ field associated with the current loop in Fig 10a; a convenient choice is to take only $\mathcal{B}_{a\tau}$ non-zero along the links which pierce the current loop in Fig 10a. Including the additional offset $\mathcal{B}_{a\mu}$, we can continue the analysis of Eq. (4.29) as before, and obtain an expression corresponding to that in Eq. (4.6).

We now split the $b_{a\sigma\mu}$ gauge fields into its uniform and staggered components as in Eq. (4.10). Manipulating the expressions in the action in Eq. (4.29) we find that they can be split into those involving the uniform ($A_{a\mu}$) and staggered ($C_{a\mu}$) components respectively. While the resulting action has decoupled contributions from $A_{a\mu}$ and $C_{a\mu}$, it should be kept in mind that their fluctuations are not truly independent. In particular, because the $b_{a\sigma\mu}$ must be integers, the $A_{a\mu}$ and $C_{a\mu}$ must *both* be either integers or half-integers. As we argue below, the $A_{a\mu}$ field fluctuates strongly in the superfluid phase (so that it can effectively be considered a continuous real field), and so it appears reasonable to ignore such a constraint. However it is possible we are overlooking some subtlety here, and it may be worthwhile to re-examine this issue in future work.

For the uniform component we obtain the terms in the action

$$\mathcal{S}_A[J] = \frac{1}{4e^2} \sum_a (2\epsilon_{\mu\nu\lambda}\Delta_\nu A_{a\lambda} + J_{31\mu} + J_{42\mu} - 2H\delta_{\mu\tau})^2. \quad (4.32)$$

Notice that the source term here is the sum of the two currents flowing from one pair field to the other, and so upon coarse-graining it looks like the current of a charge 2 object (*i.e.* a Cooper pair) moving between 12 and 34. In the superfluid phase, the uniform gauge field $A_{a\mu}$ is in its Coulomb phase because the vortex fields $\psi_{a\sigma}$ are gapped. So we can easily evaluate the expectation value of the action in Eq. (4.32) by treating $A_{a\mu}$ as a real variable controlled by the usual Maxwell action. In this manner we deduce that the contribution of the uniform component of the gauge field to G_{1234} is

$$\begin{aligned} \frac{\int \mathcal{D}A_{a\mu} e^{-\mathcal{S}_A[J]}}{\int \mathcal{D}A_{a\mu} e^{-\mathcal{S}_A[0]}} &= \\ \exp\left(\left(\Delta_\mu(J_{31\mu} + J_{42\mu})\right) \frac{1}{-4e^2\Delta_\lambda^2} \left(\Delta_\nu(J_{31\nu} + J_{42\nu})\right)\right). \end{aligned} \quad (4.33)$$

The divergence of the currents is only non-zero at the location of the Cooper pair source terms, and so we see that the correlator is the magnetic energy of two ‘monopole’

sources at these locations. The square root of this correlator in the limit of infinite separation is the superfluid order parameter, and this is given by the finite self-energy of a single monopole. In addition, there is a $1/r$ interaction between the monopoles, and this power-law decay arises from the superflow fluctuations in the dual superfluid.

We turn next to the contribution of the staggered field $C_{a\mu}$ to the action in Eq. (4.29). In the gauge $N_a = 0$, the relevant contribution to the action is

$$\begin{aligned} \mathcal{S}_C[J] &= \frac{g}{2} \sum_a (\mathcal{B}_{a\mu} + \mathcal{X}_{a\mu} - 2C_{a\mu})^2 \\ &\quad + i\pi \sum_a (\mathcal{B}_{a\tau} + \mathcal{X}_{a\tau} - 2C_{a\tau}) \\ &\quad + \frac{1}{4e^2} \sum_a (2\epsilon_{\mu\nu\lambda}\Delta_\nu C_{a\lambda} + J_{31\mu} + J_{24\mu} - 2\eta_i W\delta_{\mu\tau})^2. \end{aligned} \quad (4.34)$$

We now shift $2C_{a\mu}$ by $\mathcal{B}_{a\mu} + \mathcal{X}_{a\mu}$, and using Eqs. (4.5) and (4.31) the action above can be written as

$$\begin{aligned} \mathcal{S}_C[J] &= 2g \sum_a C_{a\mu}^2 - 2i\pi \sum_a C_{a\tau} \\ &\quad + \frac{1}{4e^2} \sum_a \left(2\epsilon_{\mu\nu\lambda}\Delta_\nu C_{a\lambda} - J_{12\mu} - J_{43\mu} \right. \\ &\quad \left. - \eta_i(2W + 1)\delta_{\mu\tau}\right)^2. \end{aligned} \quad (4.35)$$

The most important property of this expression is that it only involves the local currents $J_{12\mu}$ and $J_{43\mu}$ which are entirely localized at the Cooper pair source terms. So when these sources move far apart, the correlator factorizes into two contributions, one for each order parameter insertion. Furthermore, because the staggered gauge correlations of Eq. (4.11) decay exponentially with separation, it follows that these insertions can be evaluated independently of each other. As discussed earlier, this is indicative of ODLRO.

Next consider the dependence of $G_{12;34}$ upon 34, keeping 12 fixed and far away. For two sets of points 34 and 3'4', one has

$$\frac{G_{12;34}}{G_{12;3'4'}} = \frac{\sum_{C_{a\mu}} e^{-S_C[J_{12}, J_{34}]}}{\sum_{C_{a\mu}} e^{-S_C[J_{12}, J_{3'4'}]}} \quad (4.36)$$

For large g , one clearly sees that the numerator and denominator are dominated by $C_{a\mu} = 0$, independently of J_{34} and $J_{3'4'}$. Hence there is no directional or other dependence of $G_{12;34}$ on either pair of points, and we can conclude that $G_{12;34}$ reaches a featureless constant in the superfluid phase as 12 and 34 move apart from each other. The pairing signature in Eq. (4.26) is determined by the μ_α , as promised.

V. COLLECTIVE $S = 1$ ‘TRIPLON’ EXCITATIONS

We discussed the inclusion of non-zero spin excitations in the dimer model in Section III, but focused entirely

on fermionic $S = 1/2$ degrees of freedom. We also noted in Section III B that neutral $S = 1/2$ excitations did not survive in the insulator: instead they confined in pairs to create stable, bosonic $S = 1$ ‘triplon’ excitations. It is to this triplon excitation that we now turn our attention to. In principle, the triplon can also survive as a stable excitation into the supersolid or superfluid phases, provided energy and momentum conservation constraints prevent its decay into pairs of $S = 1/2$ Bogoliubov quasiparticles.

Microscopically, we can also see the necessity of including the triplon excitation by referring to previous analyses using bond operators^{14,22,23}. As discussed therein, two electrons on sites at the ends of a square lattice link, in addition to forming a spin singlet valence bond (a dimer), can also be in a higher energy $S = 1$ combination. It is the motion of this $S = 1$ state that we wish to examine here.

Clearly, establishing the stability of the triplon requires an accounting of fluctuations of the compact $U(1)$ gauge field $\hat{\mathcal{A}}$. So we need to work with dual fields of Section IV to account for the $S = 0$ sector. It is cumbersome to carry triplon through this duality analysis, and so we will attempt to guess its effective action using symmetry considerations.

Our approach will be to combine the approach of Ref. 24 with the results of I and of Section IV. As in Ref. 24, we represent the triplon by a real vector field \vec{n}_i , where the arrow denotes a vector in spin space. The spin operator on site j is related to \vec{n}_j by

$$\vec{S}_j \propto \eta_i \vec{n}_j ; \quad (5.1)$$

so, on its own, \vec{n}_i is a measure of spin correlations at the commensurate antiferromagnetic wavevector (π, π) . Given the short range antiferromagnetic couplings between the spins (or, alternatively, using the results the microscopic calculation of Ref. 14), we follow Ref. 24 in postulating the following phenomenological quantum lattice model for the \vec{n}_i :

$$\begin{aligned} \mathcal{S}_{n0} = & \int d\tau \sum_j \left[\frac{1}{2} \left(\frac{\partial \vec{n}_j}{\partial \tau} \right)^2 + \frac{s}{2} \vec{n}_j^2 + \frac{u}{4} (\vec{n}_j^2)^2 \right] \\ & + \int d\tau \sum_{\langle jj' \rangle} \frac{c^2}{2} (\vec{n}_j - \vec{n}_{j'})^2 . \end{aligned} \quad (5.2)$$

Here s is a parameter which determines the gap towards triplon excitations, u is a quartic non-linearity, and c is a velocity. In the absence of any coupling to the $S = 0$ charged excitations, Eqs. (5.1), (5.2) predict that the the lowest energy triplon excitation is at wavevector (π, π) .

It is now useful to characterize universal aspects of the vortex theory of Section IV using the methods of I. From I we learn that for $f = \tilde{p}/\tilde{q}$ (\tilde{p} , \tilde{q} relatively prime integers), the low energy physics of the $S = 0$ sector is captured by \tilde{q} vortex fields φ_ℓ , $\ell = 0, 1 \dots (\tilde{q} - 1)$. The effective action for the φ_ℓ fields is as described in I. From these vortex

fields we can also construct the density operators

$$\rho_{mn} = \omega^{mn/2} \sum_{\ell=0}^{\tilde{q}-1} \varphi_\ell^* \varphi_{\ell+n} \omega^{\ell m}, \quad (5.3)$$

where m, n are integers, representing Fourier components of ‘density’-like observables (such as pairing amplitude, exchange energy, or site charge density) at wavevector $2\pi f(m, n)$. Finally, from the ρ_{mn} we can Fourier transform to real space and obtain $\delta\rho(\mathbf{r})$, the value the ‘density’ at the sites, links, and plaquettes of the square lattice; the manner in which this is done, and the conventions for \mathbf{r} , are described below and in Eq. (2.26) of I.

We can now compute the effect of the $S = 0$ sector on the triplon \vec{n} excitation just as in Ref. 24. We assume that the variations in $\delta\rho(\mathbf{r})$ modulate the exchange constants between (and the amplitudes of) the \vec{n}_j , and so write down the simplest local couplings between these degrees of freedom:

$$\begin{aligned} \mathcal{S}_{n1} = & \int d\tau \sum_j \left[\lambda_1 \delta\rho(\mathbf{r}_j) \vec{n}_j^2 \right. \\ & + \lambda_2 \sum_\alpha \delta\rho(\mathbf{r}_{j+\hat{e}_\alpha/2}) \vec{n}_j \cdot \vec{n}_{j+\hat{e}_\alpha} \\ & \left. + \lambda_3 \sum_\alpha \delta\rho(\mathbf{r}_j) \vec{n}_{j-\hat{e}_\alpha} \cdot \vec{n}_{j+\hat{e}_\alpha} + \dots \right] \end{aligned} \quad (5.4)$$

We can now analyze $\mathcal{S}_{n0} + \mathcal{S}_{n1}$ as in Refs. 22,23,24. For static condensed φ_ℓ , as obtains in a commensurate Mott insulator, we have a corresponding static modulation in $\delta\rho(\mathbf{r})$. Its influence on the triplon excitation spectrum can be as computed in Ref. 24. As was shown there, simple and natural choices for the modulations agree with neutron scattering observations^{25,26,27,28} over a wide energy range. We leave for future work the extension of these results to the case where the φ_ℓ are fluctuating.

VI. CONCLUSIONS

The primary purpose of this paper was to present a complete treatment of the interplay between VBS order and superconductivity in a model of a doped $S = 1/2$ quantum antiferromagnet on the square lattice. We aimed to do this in an approach which properly accounted for strong gauge fluctuations even at non-zero hole concentrations, δ . While numerous previous studies have studied the properties of effective gauge theories of quantum antiferromagnets, essentially all have treated gauge fluctuations only at $\delta = 0$ (see however Ref. 29). As we recall briefly below, several key characteristics of our theory were special to $\delta = 0$.

Our analysis here was carried out in the context of the doped quantum dimer model⁷, which served as a convenient effective theory for the spin $S = 0$ sector. By a duality analysis of this model in Section IV, we obtained a dual theory of vortices in the local paired-electron superconducting order. As in a previous paper¹ (referred to

as I) on pure boson models, we found that these vortices appeared in $\tilde{q} > 1$ ‘flavors’ determined by the electron-pair density in a proximate Mott insulator with $\delta \neq 0$. There is much evidence in the cuprates that they are proximate to a Mott insulator with hole density $\delta = 1/8$, and by Eq. (4.20) this translates into a value $\tilde{q} = 16$. With the knowledge of \tilde{q} , we can then freely borrow over essentially all of the results of I on the fluctuations of superflow and charge/VBS order across superconducting, supersolid, and insulating phases. The \tilde{q} vortices transform under projective representation of the square lattice space group (PSG) which strongly constrains their effective action. Any impurity-induced pinning of a vortex also induces VBS/charge order by breaking the PSG among the \tilde{q} vortices. We presented a number of results on features of impurity induced pinning of vortices in I, and the present paper has provided the promised justification for their application to scanning tunnelling microscopy (STM) experiments on the cuprates.^{30,31,32,33,34}

We also showed how the framework of the quantum dimer model could be extended to include fermionic and non-zero spin excitations. This led us to an unexpected, and fairly explicit, connection between the dimer model and previous^{9,10,11,12} slave-particle U(1) and SU(2) gauge theories of quantum antiferromagnets. This connection was established in the context of mean-field saddle points in which all gauge fluctuations were quenched. Our present analysis makes it quite clear that neglect of such gauge fluctuations is dangerous at least at small δ : all the PSG properties of vortices described in the previous paragraph emerged upon a careful treatment of such fluctuations at $\delta \neq 0$.

The relationship between these different approaches to quantum antiferromagnets is neatly highlighted by the key constraint equation in Eq. (3.33)

$$\Delta_\alpha \hat{E}_{i\alpha} + b_{i+}^\dagger b_{i+} - b_{i-}^\dagger b_{i-} + \sum_s d_{is}^\dagger d_{is} = 1, \quad (6.1)$$

obeyed at every site of the lattice. Here $\hat{E}_{i\alpha}$ is the integer-valued electric field of a compact U(1) gauge field which is a measure of the number of singlet valence bonds on a link of the direct square lattice. The $b_{i\pm}$ are bosons representing holes which carry opposite gauge charges, and the d_{is}^\dagger are $S = 1/2$ fermionic spinon degrees of freedom. (It must be emphasized that this is merely a kinematic description of theory, and the ultimate quantum numbers of the emergent quasiparticles may well be different.) In the SU(2) gauge-theoretic approaches of Refs 11,12, the first valence bond term in Eq. (6.1) is not explicitly included, although it will be generated upon renormalizing the theory to a lower energy scale; the constraint is satisfied primarily by a half-filled band of d fermions. In our present dimer model approach, in

contrast, the fluctuating electric field term plays a central role in Eq. (6.1); furthermore, we perform our duality analysis about a fermionic vacuum in which there are two and zero d fermions (for an average of one) on the two sublattices respectively (the PSG ensures that this choice of vacuum actually breaks no symmetries). Alternatively stated in more physical terms, the previous analyses^{11,12} were carried out about a background of fermions occupying a half-filled band of single-particle states, while our duality analysis assumes that the electrons are primarily in paired singlet valence bond states. The consistency of our approach with the modulations observed in STM studies of the vortex lattice³⁰ (discussed above), and the absence (so far) of the staggered current patterns near vortices predicted by the SU(2) gauge theory,³⁵ may tentatively be regarded as experimental evidence in support of the approach advocated in I and the present paper.

While our duality analysis is best controlled when the fermionic $S = 1/2$ quasiparticle excitations of the superconductor are fully gapped, the structure of our theory does allow these quasiparticles to acquire a gapless nodal structure in a superconductor, without a strong qualitative impact on any of the phases of our theory. Upon decreasing δ from deep in the superconducting state, such nodal quasiparticles can annihilate in pairs across a reduced Brillouin zone boundary in a superconductor at $\delta = \delta_f$, as has been described in previous work^{13,14,20}. Alternatively, one can imagine that the nodal quasiparticles persist in the superconducting phase right down to the Mott insulator-to-superconductor transition: the theory of I will clearly not apply to such a transition, and obtaining the correct theory for this case remains an important open problem.

Acknowledgments

We thank M. P. A. Fisher, E. Fradkin, S. Kivelson, T. Senthil, and X.-G. Wen for valuable discussions. In particular, conversations with T. Senthil stimulated us to discuss the relative contributions of the electric field and fermion density to the constraints in Eqs. (3.25), (3.33), (3.48), and (6.1). This research was supported by the National Science Foundation under grants DMR-9985255 (L. Balents), DMR-0098226 (S.S.), and DMR-0210790, PHY-9907949 at the Kavli Institute for Theoretical Physics (S.S.), the Packard Foundation (L. Balents), the Deutsche Forschungsgemeinschaft under grant BA 2263/1-1 (L. Bartosch), and the John Simon Guggenheim Memorial Foundation (S.S.). S.S. thanks the Aspen Center of Physics for hospitality. K.S. thanks S. M. Girvin for support through ARO grant 1015164.2.J00113.627012.

¹ L. Balents, L. Bartosch, A. Burkov, S. Sachdev, and K. Sengupta, cond-mat/0408329; this companion paper is

referred to as I in the text.

- ² D. S. Rokhsar and S. A. Kivelson, Phys. Rev. Lett. **61**, 2376 (1988).
- ³ N. Read and S. Sachdev, Phys. Rev. Lett. **62**, 1694 (1989); Phys. Rev. B **42**, 4568 (1990).
- ⁴ S. Sachdev, Phys. Rev. B **40**, 5204 (1989).
- ⁵ P. W. Leung, K. C. Chiu, and K. J. Runge, Phys. Rev. B **54**, 12938 (1996).
- ⁶ R. Moessner and S. L. Sondhi, Phys. Rev. B **63**, 224401 (2001).
- ⁷ E. Fradkin and S. A. Kivelson, Mod. Phys. Lett. B **4**, 225 (1990).
- ⁸ S. Sachdev and M. Vojta, J. Phys. Soc. Jpn. **69**, Suppl. B, 1 (2000), cond-mat/9910231.
- ⁹ G. Baskaran and P. W. Anderson, Phys. Rev. B **37**, R580 (1988).
- ¹⁰ S. Sachdev and N. Read, Int. J. Mod. Phys. B **5**, 219 (1991), cond-mat/0402109.
- ¹¹ X.-G. Wen and P. A. Lee, Phys. Rev. Lett. **76**, 503 (1996); Phys. Rev. Lett. **80**, 2193 (1998).
- ¹² P. A. Lee, N. Nagaosa, T.-K. Ng, and X.-G. Wen, Phys. Rev. B **57**, 6003 (1998).
- ¹³ M. Vojta and S. Sachdev, Phys. Rev. Lett. **83**, 3916 (1999); M. Vojta, Y. Zhang, and S. Sachdev, Phys. Rev. B **62**, 6721 (2000).
- ¹⁴ K. Park and S. Sachdev, Phys. Rev. B **64**, 184510 (2001).
- ¹⁵ M. Vojta, Phys. Rev. B **66**, 104505 (2002).
- ¹⁶ X.-G. Wen Phys. Rev. B **65**, 165113 (2002).
- ¹⁷ J. M. Tranquada, J. D. Axe, N. Ichikawa, A. R. Moodenbaugh, Y. Nakamura, and S. Uchida, Phys. Rev. Lett. **78**, 338 (1997).
- ¹⁸ R. Moessner, S. L. Sondhi, and E. Fradkin, Phys. Rev. B **65**, 024504 (2002).
- ¹⁹ L. S. Borkowski and C. A. R. Sa de Melo, cond-mat/9810370.
- ²⁰ M. Granath, V. Oganesyan, S. A. Kivelson, E. Fradkin, and V. J. Emery, Phys. Rev. Lett. **87**, 167011 (2001).
- ²¹ The duality analysis of Section IV is carried out with respect to the f fermion vacuum, in that the f fermion contribution to the l.h.s. of Eq. (3.25) is neglected. Note, however, that this vacuum does contain a large density of d fermions: from Eq. (3.32), we see that there are two d fermions on every site of the $\eta_i = -1$ sublattice (for an average density of one d fermion per site), and this is an important contribution to Eq. (3.33). Although the d fermion contribution appears to break the translational symmetry of the lattice, the PSG ensures that all physical observables of this saddle point preserve all square lattice symmetries. The SU(2) gauge theory saddle points of Refs. 11,12 also have an average density of one d fermion per site on the l.h.s. of Eq. (3.48), but this is realized in an explicitly translationally invariant manner by a half-filled band of d fermions.
- ²² M. Vojta and T. Ulbricht, Phys. Rev. Lett. **93**, 127002 (2004).
- ²³ G. S. Uhrig, K. P. Schmidt, and M. Grüninger, cond-mat/0402659.
- ²⁴ M. Vojta and S. Sachdev, cond-mat/0408461.
- ²⁵ J. M. Tranquada, H. Woo, T. G. Perring, H. Goka, G. D. Gu, G. Xu, M. Fujita, and K. Yamada, Nature **429**, 534 (2004).
- ²⁶ V. Hinkov, S. Pailhes, P. Bourges, Y. Sidis, A. Ivanov, A. Kulakov, C. T. Lin, D. P. Chen, C. Bernhard, and B. Keimer, Nature **430**, 650 (2004).
- ²⁷ C. Stock, W. J. L. Buyers, R. A. Cowley, P. S. Clegg, R. Coldea, C. D. Frost, R. Liang, D. Peets, D. Bonn, W. N. Hardy, and R. J. Birgeneau, cond-mat/0408071.
- ²⁸ S. M. Hayden, H. A. Mook, P. Dai, T. G. Perring, and F. Dogan, Nature **429**, 531 (2004).
- ²⁹ Z. Tešanović, Phys. Rev. Lett. **93**, 217004 (2004); A. Melikyan and Z. Tešanović, cond-mat/0408344.
- ³⁰ J. E. Hoffman, E. W. Hudson, K. M. Lang, V. Madhavan, S. H. Pan, H. Eisaki, S. Uchida, and J. C. Davis, Science **295**, 466 (2002).
- ³¹ A. Fang, C. Howald, N. Kaneko, M. Greven, and A. Kapitulnik, cond-mat/0404452.
- ³² M. Vershinin, S. Misra, S. Ono, Y. Abe, Y. Ando, and A. Yazdani, Science **303**, 1995 (2004).
- ³³ K. McElroy, D.-H. Lee, J. E. Hoffman, K. M. Lang, E. W. Hudson, H. Eisaki, S. Uchida, J. Lee, and J. C. Davis, cond-mat/0404005.
- ³⁴ T. Hanaguri, C. Lupien, Y. Kohsaka, D.-H. Lee, M. Azuma, M. Takano, H. Takagi, and J. C. Davis, Nature **430**, 1001 (2004).
- ³⁵ P. A. Lee, and X.-G. Wen, Phys. Rev. B **63**, 224517 (2001); J.-I. Kishine, P. A. Lee, and X.-G. Wen, Phys. Rev. B **65**, 064526 (2002); T. Senthil and P. A. Lee, cond-mat/0406066.